

# Ocean Alkalinity Enhancement - Avoiding runaway $\text{CaCO}_3$ precipitation during quick and hydrated lime dissolution

5 Charly A. Moras<sup>1,\*</sup>, Lennart T. Bach<sup>2</sup>, Tyler Cyronak<sup>3</sup>, Renaud Joannes-Boyau<sup>1</sup>, Kai G. Schulz<sup>1</sup>

<sup>1</sup>Faculty of Science and Engineering, Southern Cross University, Lismore, NSW, Australia

<sup>2</sup>Institute for Marine and Antarctic Studies, Ecology & Biodiversity, University of Tasmania, Hobart, TAS, Australia

<sup>3</sup>Department of Marine and Environmental Sciences, Nova Southeastern University, Fort Lauderdale, FL, USA

\* Correspondence to: Charly A. Moras ([c.moras.10@student.scu.edu.au](mailto:c.moras.10@student.scu.edu.au))

10

15

20

25

30

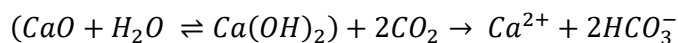
**Abstract.** Ocean Alkalinity Enhancement (OAE) has been proposed as a method to remove carbon dioxide ( $\text{CO}_2$ ) from the atmosphere and to counteract ocean acidification. It involves the dissolution of alkaline minerals ~~such as quick lime,  $\text{CaO}$ , and hydrated lime,  $\text{Ca}(\text{OH})_2$ , however~~ However, a critical knowledge gap exists regarding their dissolution in natural seawater. Particularly, how much alkaline mineral can be dissolved before secondary precipitation of calcium carbonate ( $\text{CaCO}_3$ ) occurs is yet to be established. Secondary precipitation should be avoided as it reduces the atmospheric  $\text{CO}_2$  uptake potential of OAE. ~~Here~~ Using two proposed OAE minerals as example, i.e., quick lime ( $\text{CaO}$ ) and hydrated lime ( $\text{Ca}(\text{OH})_2$ ), we show that both  ~~$\text{CaO}$  and  $\text{Ca}(\text{OH})_2$  powders~~ feedstocks ( $\Rightarrow$   $< 63 \mu\text{m}$  of diameter) dissolved in seawater within a few hours. However, while no  $\text{CaCO}_3$  precipitation, in the form of aragonite, occurred was found to occur at a saturation state ( $\Omega_{\text{Ar}}$ ) threshold of about 5,  $\text{CaCO}_3$  precipitated in the form of aragonite beyond a threshold of 7. This limit is much lower than what would be expected for typical pseudo-homogeneous precipitation in the presence of colloids and organic materials. Secondary precipitation at unexpectedly low  $\Omega_{\text{Ar}}$  was the result of so-called heterogeneous precipitation onto mineral phases, most likely onto  $\text{CaO}$  and  $\text{Ca}(\text{OH})_2$  prior to full dissolution. Most importantly, this led to runaway  $\text{CaCO}_3$  precipitation, by which i.e., significantly more alkalinity (TA) was removed than initially added, until  $\Omega_{\text{Ar}}$  reached levels below 2. Such runaway precipitation would reduce the  $\text{CO}_2$  uptake efficiency from about 0.8 moles of  $\text{CO}_2$  per mole of TA down to only 0.1 mole of  $\text{CO}_2$  per mole of TA. Runaway precipitation appears to be avoidable by dilution below the critical  $\Omega_{\text{Ar}}$  threshold of 5, ideally within hours of the addition to minimise initial  $\text{CaCO}_3$  precipitation. Finally, ~~model considerations~~ OAE simulations suggest that for the same  $\Omega_{\text{Ar}}$  threshold, the amount of TA that can be added to seawater would be more than three times higher at  $5^\circ\text{C}$  than at  $30^\circ\text{C}$ ; Also, and that equilibration to atmospheric  $\text{CO}_2$  levels, i.e., to a  $\text{pCO}_2$  of  $\sim 416 \mu\text{atm}$ , during mineral dissolution would further increase it by a factor of  $\sim 6$  and  $\sim 3$  respectively.

## 1 Introduction

Climate change is currently considered one of the ~~largest-greatest~~ threats to humankind (Hoegh-Guldberg et al., 2019; IPCC, 2021; The Royal Society and Royal Academy of Engineering., 2018). Global mean temperature ~~have~~ increased by 1.0 °C since pre-industrial times, and could reach +1.2-1.9 °C in the next 20 years, and +2.1-5.7 °C by the end of this century (IPCC, 2021). Furthermore, up to 30% of anthropogenic CO<sub>2</sub> emissions have been taken up by the ocean through air-sea gas exchange, leading to a decrease in the average open ocean pH ~~of-by~~ 0.1 units in a process termed ocean acidification – OA (Bates et al., 2012; Canadell et al., 2007; Carter et al., 2019; Cyronak et al., 2014; Doney et al., 2009; Hoegh-Guldberg et al., 2007).

The CO<sub>2</sub> reduction pledges by the signatory states of the 2015 Paris Agreement aim to ~~limit-minimise~~ the negative impacts of global warming and OA on ecosystems and human societies by limiting warming to less than +2.0 °C, ideally ~~around-below~~ +1.5 °C, by the end of this century (Goodwin et al., 2018). However, current and pledged reductions will likely not be enough and additional mitigation strategies are being discussed, such as ocean alkalinity enhancement – OAE (Boyd et al., 2019; Gattuso et al., 2015; Lenton and Vaughan, 2009; The Royal Society and Royal Academy of Engineering., 2018). ~~Among carbon dioxide removal approaches,~~ OAE ~~has a is one with the~~ highest carbon dioxide removal potential, ~~with and~~ ~~modelling-models suggests-suggesting~~ that ~~at a global scale,~~ between ~~264165~~ and 790 Gigatonnes (1 Gt = 1e1~~52~~ kg) of atmospheric CO<sub>2</sub> could be removed by 2100 ~~on a global scale-(Feng et al., 2017)~~ (Burt et al., 2021; Feng et al., 2017; Keller et al., 2014; Köhler et al., 2013; Lenton et al., 2018). ~~However, there is no empirical base on OAE efficacies, in particular regarding safe thresholds for mineral dissolution~~ (National Academies of Sciences and Medicine, 2021).

OAE typically relies on the dissolution of alkaline minerals in seawater, ~~releasing alkalinity similarly to-what occurs during~~ natural rock weathering (Kheshgi, 1995). ~~In this regard,~~ ~~Suitable candidates are~~ magnesium-rich minerals such as brucite, periclase or forsterite, and calcium-rich minerals such as quick and hydrated lime ~~have been considered~~ (Renforth and Henderson, 2017). ~~The last two minerals~~ ~~Quick and hydrated lime~~ are of particular interest, due to their high solubility in seawater as well as their relatively rapid dissolution. Quick lime, also known as calcium oxide (CaO), is obtained by the calcination of limestone, mainly composed of calcium carbonate (CaCO<sub>3</sub>) and present in large quantities in the Earth's crust (~~Kheshgi, 1995~~). Once heated to temperatures of ~1200 °C, each molecule of CaCO<sub>3</sub> breaks down into one molecule of CaO and one molecule of CO<sub>2</sub> (Ilyina et al., 2013; Kheshgi, 1995). ~~Hence, for maximum OAE potential, carbon capture during calcination and subsequent storage would be advisable~~ (Bach et al., 2019; Ilyina et al., 2013; Kheshgi, 1995; Renforth et al., 2013; Renforth and Kruger, 2013). CaO can then be hydrated into ~~hydrated lime, also known as~~ calcium hydroxide (Ca(OH)<sub>2</sub>), ~~also known as hydrated lime-(Kheshgi, 1995)~~. The addition of either CaO or Ca(OH)<sub>2</sub> to seawater leads to the dissociation of Ca(OH)<sub>2</sub> into one calcium Ca<sup>2+</sup> and two hydroxyl ions OH<sup>-</sup> (Feng et al., 2017; Harvey, 2008). ~~The chemical reaction of CaO and Ca(OH)<sub>2</sub> dissolution can be written as follow, which including includes~~ the subsequent ~~oceanic~~ uptake of atmospheric CO<sub>2</sub>, and ~~ignores~~ the non-linearities of the seawater carbonate system, (i.e., changes in total alkalinity, TA, and dissolved inorganic carbon, DIC, are not 1:1); ~~a conceptual model of CaO and Ca(OH)<sub>2</sub> dissolution can be summarised as per:~~



1

65

~~This (Renforth et al., 2013; Renforth and Kruger, 2013)~~

70

~~The dissolution of CaO and Ca(OH)<sub>2</sub> and the subsequent addition of TA chemical equation suggests that each mole of CaO or Ca(OH)<sub>2</sub> reacts with two moles of CO<sub>2</sub> to produce one mole of Ca<sup>2+</sup> and two moles of bicarbonate ions (HCO<sub>3</sub><sup>-</sup>). A different way to look at this is that adding Ca<sup>2+</sup> to seawater increases TA by two moles per mole of Ca<sup>2+</sup>, while leaving the concentration of DIC unchanged (Wolf Gladrow et al., 2007). This increases the pH, lowering the CO<sub>2</sub> concentration, [CO<sub>2</sub>], and increasing the carbonate ion concentration, [CO<sub>3</sub><sup>2-</sup>] increases seawater pH, while changing the carbonate chemistry speciation. DIC can be approximated by being the sum of HCO<sub>3</sub><sup>-</sup> and CO<sub>3</sub><sup>2-</sup> (ignoring the relatively small contribution by CO<sub>2</sub>). Similarly, TA can be approximated as the sum of HCO<sub>3</sub><sup>-</sup> and 2 CO<sub>3</sub><sup>2-</sup> (ignoring the smaller contributions by boric and silicic acid, and other minor components). Combining both DIC and TA equations reveal that CO<sub>3</sub><sup>2-</sup> concentrations can be expressed as [CO<sub>3</sub><sup>2-</sup>] = TA-DIC. Hence, increasing TA at constant DIC, e.g., by dissolving CaO or Ca(OH)<sub>2</sub>, increases [CO<sub>3</sub><sup>2-</sup>], shifting carbonate chemistry speciation towards higher pH (Figure A 1 Figure A 1, Appendix) (Dickson et al., 2007; Wolf-Gladrow et al., 2007; Zeebe and Wolf-Gladrow, 2001). This in turn The shift in DIC speciation leads to a decrease in [CO<sub>2</sub>], reduces reducing the partial pressure of CO<sub>2</sub> (pCO<sub>2</sub>) in seawater and increasing its atmospheric CO<sub>2</sub> uptake -potential.~~

75

80

~~Depending on the amount of TA added and the initial seawater pCO<sub>2</sub>, the TA-enriched seawater would either take up CO<sub>2</sub> from the atmosphere or degas less until equilibrium is restored, hence acting as a sink for atmospheric CO<sub>2</sub> reduce outgassing of CO<sub>2</sub> in the case where seawater pCO<sub>2</sub> is still above atmospheric levels. Factoring in carbonate system non-linearities, about 1.6 moles of atmospheric CO<sub>2</sub> could be taken up per mole of CaO or Ca(OH)<sub>2</sub> (Köhler et al., 2010). Furthermore, dissolving CaO and Ca(OH)<sub>2</sub> can also counteract OA ocean acidification in two ways, raising the pH of seawater and raising the calcium carbonate saturation state of seawater (Ω<sub>CaCO<sub>3</sub></sub>), with Ω<sub>CaCO<sub>3</sub></sub> increasing both because of increased by increasing both dissolved [Ca<sup>2+</sup>] and [CO<sub>3</sub><sup>2-</sup>]. Therefore, This makes OAE is a dual solution for both removing CO<sub>2</sub> from the atmosphere and changing ocean acidification trajectory removing atmospheric CO<sub>2</sub> and mitigating OA (Boyd et al., 2019; Feng et al., 2017; Harvey, 2008). However, major knowledge gaps exist regarding OAE, considering most research to date has been based on conceptual and numerical modelling (Feng et al., 2016; González and Ilyina, 2016; Mongin et al., 2021; Renforth and Henderson, 2017).~~

85

90

~~One such knowledge gap of the major constraints is keeping CaCO<sub>3</sub> saturation state (Ω) of the seawater below a the critical Ω<sub>CaCO<sub>3</sub></sub> critical threshold; that seawater can be raised to beyond which CaCO<sub>3</sub> would precipitate inorganically. Such secondary precipitation constitutes the opposite of alkaline mineral dissolution and would decrease pH and Ω<sub>CaCO<sub>3</sub></sub>, simultaneously increasing increase seawater [CO<sub>2</sub>] through decreasing [CO<sub>3</sub><sup>2-</sup>]. This would decrease the ocean uptake's capacity for atmospheric CO<sub>2</sub>, and if having the opposite effect of what is initially intended. Similarly, if all added alkalinity is being precipitated, only 1 mole of atmospheric CO<sub>2</sub> per mole of Ca<sup>2+</sup> would be removed, instead of about 1.6 without. If even more CaCO<sub>3</sub> precipitates, the efficiency would be further reduced.~~

95

CaCO<sub>3</sub> does not precipitate spontaneously in typical seawater due to various factors such as the absence of mineral phase precipitation nuclei and the presence of precipitation inhibitors such as dissolved organic compounds, magnesium or phosphate (Chave and Suess, 1970; De Choudens-Sanchez and Gonzalez, 2009; Pytkowicz, 1965; Rushdi et al., 1992; Simkiss, 1964).  
100 The latter two directly influence CaCO<sub>3</sub> nuclei formation rates. (Chave and Suess, 1970; Pan et al., 2021)~~The~~There are three types of precipitation, i.e., 1) homogeneous (in the absence of any precipitation nuclei), 2) heterogeneous (in the presence of mineral phases), and 3) pseudo-homogeneous (in the presence of colloids and organic materials) (Marion et al., 2009; Morse and He, 1993).~~critical threshold for  $\Omega$  with respect to the CaCO<sub>3</sub> mineral phase calcite,  $\Omega_{Ca}$ , has been determined experimentally (Marion et al., 2009) for so called pseudo homogeneous precipitation, i.e., in the presence of colloids and organic materials (Morse and He, 1993). For a salinity of 35 and at a temperature of 21 °C, t~~For the latter, the critical precipitation threshold for calcite (at a salinity of 35 and at a temperature of 21 °C) is at a saturation state ( $\Omega_{Ca}$ ) value is of ~18.8 (Marion et al., 2009).~~Marion et al. (2009).~~Assuming a typical open-ocean TA and DIC concentrations, i.e., ~2350  $\mu\text{mol kg}^{-1}$  and ~2100  $\mu\text{mol kg}^{-1}$  respectively (Dickson et al., 2007), this threshold would be reached by an increase in TA of ~810  $\mu\text{mol kg}^{-1}$ , corresponding to a critical threshold for  $\Omega_{CaCO_3}$  with respect to aragonite, i.e.,  $\Omega_{Ar}$ , of ~12.3. Concerning the  
110 ~~Furthermore, there are~~two other types of precipitation, i.e., homogeneous (in the absence of any precipitation nuclei) and heterogeneous (in the presence of mineral phases), but these thresholds are poorly constrained (Marion et al., 2009). Importantly, at the current seawater dissolved magnesium concentration, the CaCO<sub>3</sub> morphotype that is favoured during inorganic precipitation is aragonite rather than calcite (Morse et al., 1997; Pan et al., 2021).

~~A better understanding of dissolution and precipitation kinetics is needed to address knowledge gaps in OAE research. In order to do so~~To gain a better understanding, we conducted several dissolution experiments with CaO and Ca(OH)<sub>2</sub> ~~were carried out~~to determine 1) how much alkaline material can be dissolved without inducing CaCO<sub>3</sub> precipitation, 2) what causes secondary CaCO<sub>3</sub> precipitation, and 3) how ~~it~~ secondary precipitation can be avoided if observed.

## 2 Material & Methods

### 2.1 Experimental setup

120 Two different calcium minerals were ~~sourced used, calcium oxide (CaO)~~ powder from Ajax Finechem (CAS no 1305-78-8) and an industrial ~~calcium hydroxide (Ca(OH)<sub>2</sub>)~~ powder (Hydrated Lime 20kg, Dingo). The elemental composition of these powders was analysed on an Agilent 7700 Inductively Coupled Plasma Mass Spectrometer, coupled to a laser ablation unit NWR213 from ESI~~Electro Scientific Industries, Inc.~~ ~~For that purpose, t~~The samples were embedded in resin and calibrated against standard reference materials #610 and #612 from the National Institute of Standards and Technology.

125 The dissolution experiments were conducted in natural seawater. The seawater was ~~sampled-collected between September 2020 and June 2021,~~ about 200 to 300 m from the shore, avoiding ~~suspended-collecting~~ sand or silt, at Broken Head, New South Wales, Australia (28°42'12" S, 153°37'03" E). ~~It~~Seawater was stored up to 14 days at 4 °C in the dark to slow bacterial metabolic activity and allow for all particles in suspension to sink to the bottom before being sterile-filtered

130 using a peristaltic pump, connected to a 0.2  $\mu\text{m}$  Whatman Polycap 75 AS filter. For salinity measurements, about 200 mL of seawater were placed in a gas-tight polycarbonate container and allowed to equilibrate to room temperature overnight. The sample's conductivity was then measured using a measuring cell (Metrohm 6.017.080), connected to a 914 pH/Conductometer. The conductivity was recorded in millisiemens per cm (mS/cm), and the temperature in  $^{\circ}\text{C}$ . Salinity was calculated according to Lewis and Perkin (1981) on the 1978 practical salinity scale. The salinity in each experiment is reported in Table A 1.

## 2.2 OAE experiments

135 For each experiment, seawater was accurately weighed (in grams to 2 decimal places) into high-quality borosilicate 3.3 L ~~or 5L~~ Schott Duran beakers, and the temperature was controlled via a Tank Chiller Line TK 1000 set to 21  $^{\circ}\text{C}$ , feeding a re-circulation water jacket (Figure A 2 ~~Figure A 2, supplementary material~~). A magnetic stir bar was placed in the beaker, and the natural seawater was constantly stirred at  $\sim 200$  rpm. To minimise gas exchange, a floating lid with various sampling ports was placed on top. Finally, after one hour of equilibration, calculated amounts of weighed-in alkaline compounds were added. Upon addition, samples for DIC and TA were taken ~~in at~~ increasing time intervals to fully capture the dissolution kinetics and check for potential secondary precipitation. Furthermore, the pH was monitored at a frequency of 1 Hertz for the first hour before alkalinity addition, and over ~~5-4~~ hours after addition to get an estimate for determine when alkalinity was fully released. Once the pH plateaued (corresponding to maximum TA release was reached), the ~~content of the beaker entire content of the beaker~~ was carefully transferred to a clean Schott bottle of the corresponding volume to ensure that evaporation would ~~not play a role in changing DIC and TA. The b~~ Bottles were kept in the dark for the duration of each experiment, i.e., up to 48 days, with the same constant stirring of  $\sim 200$  rpm at 21  $^{\circ}\text{C}$ . Each bottle was exposed to UV light for at least 30 minutes after each sampling to avoid bacterial growth.

### 2.2.1 CaO and Ca(OH)<sub>2</sub> dissolution

150 ~~The additions of sieved CaO and Ca(OH)<sub>2</sub> were performed~~ Following the previously described beaker setup, TA was added by sieving CaO and Ca(OH)<sub>2</sub> through ~~using~~ a 63  $\mu\text{m}$  mesh, ~~avoiding the formation of larger CaO or Ca(OH)<sub>2</sub> aggregates.~~ The mesh was placed in a clean upside-down 50 mL Falcon tube cap, ~~avoiding to minimise the loss losing any of~~ material smaller than 63  $\mu\text{m}$  ~~when weighing~~, and the overall weight was recorded in mg. Then, the mesh was placed above the Schott bottle, and mineral was added by gently tapping the side of the sieve. Finally, the sieve was placed in the same upside-down Falcon tube cap and ~~the weight weighed once again of the whole setup was recorded again, thereby~~ making sure that the desired amount had been added to the beaker. The weighing steps were carefully performed to avoid material loss between the bottle and the balance, and was achieved in less than 5 min. Two alkalinity additions, +250 and +500  $\mu\text{mol kg}^{-1}$  with each calcium mineral powder were performed (Table 1 ~~Table 1~~).

## 2.2.2 Na<sub>2</sub>CO<sub>3</sub> alkalinity and particles additions, and filtration

160 ~~Three further experiments assessed A~~ the role of mineral phases during secondary CaCO<sub>3</sub> precipitation observed in the previous experiments. The first experiment made use of a 1M solution of sodium carbonate (Na<sub>2</sub>CO<sub>3</sub>, CAS number 497-19-8) ~~which~~ was freshly prepared before the experiment. Ultrapure Na<sub>2</sub>CO<sub>3</sub> (~~CAS number 497-19-8~~) was accurately weighed, ~~i.e., in mg (with 2 decimal places),~~ into a clean 100 mL Schott bottle and made up to 100 g with MilliQ (18.2 MΩ). The solution was then sonicated for 15 minutes ~~with gentle shaking, and gentle mixing every five minutes.~~ The amount of Na<sub>2</sub>CO<sub>3</sub> to be added ~~to seawater~~ was calculated so that a similar maximum  $\Omega_{Ar}$  would be reached, i.e., ~7.7, as in the previous  
165 experiments with the highest addition of CaO and Ca(OH)<sub>2</sub>. This required ~~almost about~~ twice the alkalinity increase as before (~~Table 1~~ ~~Table 4~~), because Na<sub>2</sub>CO<sub>3</sub> additions concomitantly increase DIC when dissociating in two sodium ~~ions, i.e., Na<sup>+</sup>,~~ and one CO<sub>3</sub><sup>2-</sup> ~~ion,~~ making the  $\Omega_{CaCO_3}$  increase ~~smaller smaller.~~ ~~Calculations All carbonate chemistry calculations~~ were done in CO<sub>2</sub>SYS (see below).

In another, ~~otherwise identical similar,~~ experiment ~~with to~~ the Na<sub>2</sub>CO<sub>3</sub> ~~additions solution,~~ quartz powder was added after two days. ~~Quartz powder was chosen as it does not dissolve on the timescales relevant for this study~~ (Montserrat et al., 2017). The addition of quartz powder was similar to the sieved CaO and Ca(OH)<sub>2</sub> additions, i.e., through a 63 μm mesh. The ~~amount mass~~ of quartz particles added, ~~recorded in mg,~~ was determined to provide the same ~~amount of~~ mineral surface ~~area~~ as for the Ca(OH)<sub>2</sub> experiments with a TA increase of 500 μmol kg<sup>-1</sup>. It was calculated using densities and masses for Ca(OH)<sub>2</sub> and quartz, and assuming spherical particles with a diameter of 63 μm. ~~Quartz powder was chosen as it does not dissolve on timescales relevant to the experiment and hence does not supply extra TA (Montserrat et al., 2017).~~  
175

Finally, ~~a particle filtering experiment a~~ third experiment was carried out ~~in which all particles were removed by filtration,~~ using Ca(OH)<sub>2</sub> as the alkaline compound ~~and~~ following the same setup as described above (~~section 2.2.1~~). Here we first added Ca(OH)<sub>2</sub> to increase TA by ~500 μmol kg<sup>-1</sup> (~~Table 1~~ ~~Table 4~~). After 4h of reaction, the entire content of the 2L Schott beaker was filtered through a nylon Captiva Econofilter (25mm) with a pore size of 0.45 μm into a clean 1L Schott  
180 bottle using a peristaltic pump. The bottle was filled from bottom to top, with overflow to minimise gas exchange.

## 2.2.3 Dilution experiments

~~In a~~ last set of experiments, ~~diluted~~ alkalinity enriched ~~samples seawater was diluted~~ with natural seawater ~~over time,~~ to test if secondary precipitation can be avoided ~~or stopped through dilution.~~ Ca(OH)<sub>2</sub> ~~powder~~ was added to reach a final alkalinity enrichments of 500 and 2000 μmol kg<sup>-1</sup> ~~and dilutions were carried out at several points in time.~~ ~~These initial concentrations were then diluted with NSW in several steps as described in the following.~~  
185

For the experiment with a targeted TA increase of 500 μmol kg<sup>-1</sup>, ~~a larger quantity of TA enriched seawater was required to perform all dilutions and sampling in comparison to the previous experiments.~~ Therefore, two 5L Schott bottles were filled with 5kg of natural seawater and placed on a magnetic stirring platform. Calculated ~~weighed-in masses amounts of~~ Ca(OH)<sub>2</sub> were added to the first bottle ~~as described in section 2.2.1 using the 63 μm sieve,~~ while the natural seawater in the

190 second bottle was left-kept for future-subsequent dilutions. Both bottles were kept on the same bench under the same conditions, both stirring at a rate of ~200\_rpm, for the duration of the experiment. ~~Ca(OH)<sub>2</sub> powder was added as described above using the 63 μm sieve.~~ Following the Ca(OH)<sub>2</sub> addition, 1:1 dilutions (500 g TA enriched seawater:500 g natural seawater) were performed in clean 1L Schott bottles that were then kept in the dark and placed on a magnetic platform at a stirring rate of ~200\_rpm. After each sampling, the bottles were exposed to UV light for at least 30 minutes. The second dilution experiment was set up like the first one, the only difference being that the targeted TA increase was 2000 μmol kg<sup>-1</sup>. The dilution ratio was 1:7 to, ~~again,~~ reduce the targeted TA increase again to 250 μmol kg<sup>-1</sup>. All dilutions were performed 10 minutes, 1 hour, 1 day and 1 week after Ca(OH)<sub>2</sub> addition, leading to 2 TA-enriched and 8 diluted treatments.

### 2.3 Carbonate chemistry measurements

200 Samples for TA and DIC measurements were filtered through a nylon Captiva Econofilter (0.45 μm) using a peristaltic pump into 100 mL Borosilicate 3.3 Schott DURAN glass stopper bottles. The bottles were gently filled from the bottom to top, using a 14-gauge needle as described in Schulz et al. (2017), with at least half of their volume allowed to overflow, corresponding to ~150 mL of seawater sampled per time-point (Dickson et al., 2007). After filling, 50μL of saturated mercuric chloride solution was added to each sample before being stored without headspace in the dark at 4 °C. TA was analysed in duplicates via potentiometric titrations on an 848 Titrimo Plus coupled to an 869 Compact Sample Changer from Metrohm using 0.05M HCl, with the ionic strength adjusted to 0.72 mol kg<sup>-1</sup>, with NaCl, corresponding to a salinity of 35 ~~with NaCl~~. Titrations and calculations followed the open-cell titration protocols by Dickson et al. (2007). DIC was measured in triplicates using an Automated Infra-Red Inorganic Carbon Analyzer (AIRICA) coupled to a LICOR Li7000 Infra-Red detector as described in Gafar and Schulz (2018). Measured values of TA and DIC were corrected using an internal Standard prepared as per Dickson et al. (2007) which had been calibrated against Certified Reference Materials Batch #175 and #190 (Dickson, 210 2010).

### 2.4 Particulate Inorganic Carbon and Scanning Electron Microscopy (SEM)

215 In cases where TA and DIC decreases were detected, indicative of CaCO<sub>3</sub> precipitation, several samples were taken at the end of the experiments ~~Samples~~ for total particulate carbon (TPC), ~~and~~ particulate organic carbon (POC) and scanning electron microscopy (SEM) analyses. TPC and POC samples were collected in duplicates at the end of some experiments on pre-combusted (450 °C) GF/F filters, and stored frozen until analysis. ~~Then~~ Before analysis, POC filters were fumed with HCl for 2 hours before drying over night at 60 °C while TPC filters were dried untreated (Gafar and Schulz, 2018). The filters were wrapped in tin capsules and pressed into small balls of about 5mm diameter. Both TPC and POC were quantified on an Elemental Analyser Flash EA, Thermo Fisher, coupled to an Isotope Ratio Mass Spectrometer ~~(IRMS)~~, Delta V Plus. Particulate inorganic carbon (PIC), or CaCO<sub>3</sub>, was calculated from the difference between TPC and POC. The results are reported in μmol kg<sup>-1</sup> with an uncertainty estimate for each calculated by an error propagation from the square root of the sum of the squared standard deviations for TPC and POC. ~~Finally, samples of CaO and Ca(OH)<sub>2</sub> were analysed for their carbon~~

~~content. This analysis aimed to identify the presence and estimate the amount of particulate carbon, most likely CaCO<sub>3</sub>, in the respective mineral powders.~~

~~When CaCO<sub>3</sub> was suspected to have precipitated in the experiments, samples for SEM analysis were taken. For that purpose SEM analysis, 10 to 15 mL of the sample water was collected on polycarbonate Whatman Cyclopore filters with a 0.2 μm pore size, and rinsed with 50 mL of MilliQ. The filters were dried at 60 °C overnight and kept in a desiccator until analysis on a tabletop Scanning Electron Microscope TM4000 Plus from Hitachi, coupled to an Energy Dispersive X-Ray (EDX) Analyser, allowing to identify the morphotype and elemental composition of precipitates. Finally, samples of CaO and Ca(OH)<sub>2</sub> powders were analysed for their carbon content. This analysis aimed to identify the presence and estimate the amount of particulate carbon, most likely CaCO<sub>3</sub>, in the respective mineral powders.~~

## 2.5 Carbonate chemistry calculations

~~Measured DIC, TA, temperature and salinity were used to calculate the remaining carbonate chemistry seawater parameters were calculated using with the CO<sub>2</sub>SYS script for MATLAB® (MathWorks), using the The borate to salinity relationship from Uppstrom (1974), dissociation constants for carbonic acid by Lueker et al. (2000), and for boric acid by Uppstrom (1974) were used. With two measured carbonate chemistry parameters, i.e., DIC and TA, most of the others can be calculated straight away. An exception in our experiments was that the addition-dissolution of CaO and Ca(OH)<sub>2</sub> changes the calcium concentration and hence the salinity-based Ω<sub>CaCO<sub>3</sub></sub> calculated by CO<sub>2</sub>SYS is erroneous underestimated. Ω<sub>CaCO<sub>3</sub></sub> is defined by the solubility product of CaCO<sub>3</sub> as:~~

$$\Omega_{CaCO_3} = \frac{[Ca^{2+}] \times [CO_3^{2-}]}{K_{sp}} \quad 2$$

where [Ca<sup>2+</sup>] and [CO<sub>3</sub><sup>2-</sup>] denote seawater concentration of Ca<sup>2+</sup> and CO<sub>3</sub><sup>2-</sup>, and K<sub>sp</sub> the solubility product for calcite or aragonite. To calculate saturation states, ~~CO<sub>2</sub>SYS was used to determine K<sub>sp</sub> and [CO<sub>3</sub><sup>2-</sup>] from measured DIC and TA. The correct calcium concentration [Ca<sup>2+</sup>]<sub>corr</sub> was estimated from measured salinity (Riley and Tongudai, 1967) plus and half the amount of alkalinity concentration increase that was generated during CaO or Ca(OH)<sub>2</sub> dissolution or lost due to CaCO<sub>3</sub> precipitation, ΔTA:~~

$$[Ca^{2+}]_{corr} = \frac{0.02128}{40.087} \times \frac{Salinity}{1.80655} + \frac{\Delta TA}{2} \quad [Ca^{2+}]_{corr} = \frac{0.01028}{35} \times Salinity + \frac{\Delta TA}{2} \quad 3$$

~~where 0.01028 denotes molar Ca<sup>2+</sup> concentrations at a salinity of 35. K<sub>sp</sub> was calculated from in-situ temperature and salinity according to Mucci (1983). The corrected Ω<sub>Ca</sub> and Ω<sub>Ar</sub> were then calculated from in situ [CO<sub>3</sub><sup>2-</sup>], [Ca<sup>2+</sup>]<sub>corr</sub> and K<sub>sp</sub> according to Equation 2. Please note that we have opted to rather report Ω<sub>Ar</sub> rather than Ω<sub>Ca</sub> since aragonite is more likely to be~~



precipitated in natural modern seawater (Berner, 1975; Morse et al., 1997; Riebesell et al., 2011; Zeebe and Wolf-Gladrow, 2001).

## 2.6 OAE simulations

CO<sub>2</sub>SYS and the results from the various dissolution experiments were used to simulate three OAE scenarios (Table 3). Three alkalinity additions were simulated, +250, +500 and +1000  $\mu\text{mol kg}^{-1}$ . The starting parameters were TA = 2350  $\mu\text{mol kg}^{-1}$ , DIC = 2100  $\mu\text{mol kg}^{-1}$ , salinity = 35, temperature = 19 °C, using the same acid-base equilibrium constants as described in section 2.5. In the first scenario, for all three additions, no CaCO<sub>3</sub> precipitation was assumed, and the amount of CO<sub>2</sub> taken up after atmospheric re-equilibration was calculated. For the +500 and +1000  $\mu\text{mol kg}^{-1}$  TA increases, two additional simulations were performed: first we assumed that as much CaCO<sub>3</sub> precipitated as TA was added, and second, that CaCO<sub>3</sub> precipitated down to an  $\Omega_{Ar}$  of ~2 as observed in our experiments. Again, after calculating full carbonate chemistry speciation in these various scenarios, the amount of CO<sub>2</sub> taken up after atmospheric re-equilibration was determined.

## 3 Results

### 3.1 Chemical composition of CaO and Ca(OH)<sub>2</sub>

The chemical composition of the CaO and Ca(OH)<sub>2</sub> powders were analysed for their major ions. As to be expected, both consisted mainly of calcium, with minor contributions by of magnesium and silicon (see Table A 2 Table A 1, Appendix, for a more extensive-comprehensive list). Furthermore, CaO and Ca(OH)<sub>2</sub> contained about 9.4  $\pm 0.1$  mg g<sup>-1</sup> and 18.0  $\pm 0.2$  mg g<sup>-1</sup> of particulate carbon respectively, i.e., ~0.9% and ~1.8% by weight.

### 3.2 CaO dissolution in filtered natural seawater

In the first CaO experiment with a targeted ~250  $\mu\text{mol kg}^{-1}$  TA addition, TA increased by ~200  $\mu\text{mol kg}^{-1}$  within the first 4 hours (Figure 1 Figure 1a). Following this increase, TA was stable over time. In contrast, DIC increased slowly ~~over time, about 1  $\mu\text{mol kg}^{-1}$  per day~~, reaching about +50  $\mu\text{mol kg}^{-1}$  on day 47 of the experiment (Figure 1 Figure 1b). ~~Finally,  $\Omega_{Ar}$  showed a similar trend to reflected the trend observed for the  $\Delta\text{TA}$~~ , increasing from ~2.9 to ~5.1 within the first 4 hours before slowly decreasing to 5.0 as of on day 47 (Figure 1 Figure 1c).

In the second CaO experiment with about a targeted 500  $\mu\text{mol kg}^{-1}$  TA addition, TA increased by ~410  $\mu\text{mol kg}^{-1}$  within the first 4 hours before slowly decreasing on day 3 two days later (Figure 1 Figure 1a), followed by a more rapid decreases over the following week, before slowing down and eventually reaching a steady state on day 20 at a final  $\Delta\text{TA}$  of about -540  $\mu\text{mol kg}^{-1}$ . This corresponds to a total loss of TA of ~950  $\mu\text{mol kg}^{-1}$ , between the maximum measured TA and the final TA recorded. Similarly, a slight-relatively small decrease in DIC of ~10  $\mu\text{mol kg}^{-1}$  was observed over the first two days before a much more considerable-significant reduction in the following week before levelling off at a  $\Delta\text{DIC}$  of about -465

$\mu\text{mol kg}^{-1}$  (Figure 1Figure 1b). Finally,  $\Omega_{\text{Ar}}$  increased rapidly during the first 4 hours of the experiment from 2.8 up to 7.6 (Figure 1Figure 1c). Following this quick increase,  $\Omega_{\text{Ar}}$  decreased by 0.3 units by day 3. Afterwards,  $\Omega_{\text{Ar}}$  ~~within the first two days before rapidly dropping~~ dropped quickly to 2.4 on day 13, and reaching  $\sim 1.8$  on day 47, corresponding to a reduction of by 1.0 compared to the starting seawater value.

### 285 3.3 Ca(OH)<sub>2</sub> dissolution in filtered natural seawater

In the first Ca(OH)<sub>2</sub> experiment with a targeted TA addition of  $\sim 250 \mu\text{mol kg}^{-1}$ , TA increased by  $\sim 220 \mu\text{mol kg}^{-1}$  after 4h of reaction, before stabilising at a  $\Delta\text{TA}$  of  $\sim 210 \mu\text{mol kg}^{-1}$  for the rest of the experiment (Figure 2Figure 2a). The DIC concentration increased relatively quickly over the first 6 days steadily following after the TA addition before slowing down, reaching by  $\sim 70 \mu\text{mol kg}^{-1}$  until by the end of the experiment (Figure 2Figure 2b). Finally,  $\Omega_{\text{Ar}}$  reached  $\sim 4.1$  after 4  
290 hours, slightly decreasing over time, down to 3.3 on day 28 (Figure 2Figure 2c).

In the second Ca(OH)<sub>2</sub> experiment with a targeted TA addition of  $\sim 500 \mu\text{mol kg}^{-1}$ , TA increased by  $\sim 440 \mu\text{mol kg}^{-1}$  within the first 4h (Figure 2Figure 2a). This was followed by a relatively steady decrease by  $\sim 18 \mu\text{mol kg}^{-1}$  per day over the next 2 weeks, after which the decrease accelerated to  $\sim 28 \mu\text{mol kg}^{-1}$  per day until day 35, before levelling off at a  $\Delta\text{TA}$  of about  $-420 \mu\text{mol kg}^{-1}$  towards the end of the experiment. Overall, about  $\sim 860 \mu\text{mol kg}^{-1}$  of TA was lost compared to the highest  
295 TA recorded. The DIC concentration decreased as well, dropping in a similar fashion as TA and reaching a  $\Delta\text{DIC}$  of about  $-395 \mu\text{mol kg}^{-1}$  compared to the initial DIC concentration (Figure 2Figure 2b). Finally,  $\Omega_{\text{Ar}}$  increased from 2.5 to 7.4 in the first 4 hours before decreasing, similarly to TA and DIC, reaching  $\sim 2.0$  on day 42 (Figure 2Figure 2c).

### 3.4 Na<sub>2</sub>CO<sub>3</sub>, particle ~~addition filtration and filtration addition~~

Three experiments assessed the influence of particles on CaCO<sub>3</sub> precipitation. In the first one,  $\sim 1050 \mu\text{mol kg}^{-1}$  of  
300 TA was added using a 1M Na<sub>2</sub>CO<sub>3</sub> solution, designed to result in a similar maximum  $\Omega_{\text{Ar}}$  as in the previous experiments when TA precipitated-decreased (Table 1Table 1). Upon addition, TA increased by  $\sim 1060 \mu\text{mol kg}^{-1}$  and DIC by  $\sim 530 \mu\text{mol kg}^{-1}$  within minutes. For the remainder of the experiment,  $\Delta\text{TA}$  was fairly constant between 1060 and 1040  $\mu\text{mol kg}^{-1}$  (Figure 3Figure 3a). In contrast, DIC slightly increased over 42 days from a  $\Delta\text{DIC}$  of  $\sim 530 \mu\text{mol kg}^{-1}$  on day 1 to  $\sim 560 \mu\text{mol kg}^{-1}$  on day 42 (Figure 3Figure 3b). Finally,  $\Omega_{\text{Ar}}$  increased from  $\sim 2.3$  to  $\sim 8.5$  within minutes and slightly decreased to  $\sim 8.1$  after 42  
305 days of experiment (Figure 3Figure 3c).

In the second experiment, the addition of aliquots of 1M Na<sub>2</sub>CO<sub>3</sub> solution (Table 1Table 1) increased TA by 1070  $\mu\text{mol kg}^{-1}$ , while DIC increased by  $\sim 540 \mu\text{mol kg}^{-1}$  within minutes and remained stable (Figure 3Figure 3a, 3b). Then, a  
310 After 2 days, quartz particles was were added. While one day later  $\Delta\text{TA}$  and  $\Delta\text{DIC}$  remained unchanged, about a week later, between day 5 and 12  $\Delta\text{TA}$  had decreased to  $\sim 220 \mu\text{mol kg}^{-1}$  while and  $\Delta\text{DIC}$  had dropped to  $\sim 120 \mu\text{mol kg}^{-1}$  (Figure 3Figure 3a, 3b). Over the next month,  $\Delta\text{TA}$  and  $\Delta\text{DIC}$  kept on decreasing continued to decrease, although at a slowing paeerate, reaching about  $-200$  and  $-110 \mu\text{mol kg}^{-1}$ , respectively, at the end of the study. Finally,  $\Omega_{\text{Ar}}$  followed a similar trend, with an increase from

~2.8 up to ~9.2 within the first 1.5 hours, and a pronounced decline to ~3.9 between day 5 and day 12, before stabilizing around ~~to~~ ~2.0 at the end of the experiment.

In the ~~a~~ last experiment, Ca(OH)<sub>2</sub> was added aiming for a TA increase of 500 μmol kg<sup>-1</sup> (Table ~~1~~ Table 1), a level at which a significant TA decrease had been observed previously~~after 5 hours previously~~ (Figure ~~2~~ Figure 2a). In contrast however, upon filtration of the entire experimental bottle content after reaching ~470 μmol kg<sup>-1</sup> at the 4-hour mark, ΔTA remained relatively constant between 465 and 470 μmol ~~kg<sup>-1</sup>~~ kg<sup>-1</sup> over the following 48 days of experiment (Figure ~~3~~ Figure 3a). At the same time, ΔDIC increased from ~5 to 55 μmol kg<sup>-1</sup> after filtration (Figure ~~3~~ Figure 3b). ~~Finally~~, Ω<sub>Ar</sub> increased from ~2.8 to ~8.2 within the first 1.5 hours, and then slightly decreased to ~7.5 over the 48 days of experiment (Figure ~~3~~ Figure 3c).

### 3.5 Dilution experiments

#### 3.5.1 500 μmol kg<sup>-1</sup> addition

In ~~this~~~~these~~~~set of~~ experiments with a targeted TA addition of ~500 μmol kg<sup>-1</sup> by Ca(OH)<sub>2</sub>, ΔTA increased to similarly ~~to the other Ca(OH)<sub>2</sub> experiment to~~ ~450 μmol kg<sup>-1</sup> after 2 hours (Figure 4). These changes in TA were followed by a decline to ~320 μmol kg<sup>-1</sup> after 14 days, although the latter being a slightly slower decrease than previously (Figure ~~2~~ Figure 4 ~~Figure 4a, 4d~~). After a first increase in ΔDIC by ~10 μmol kg<sup>-1</sup> on day 1, ~~it~~ DIC steadily decreased to about -20 μmol kg<sup>-1</sup> after two weeks (Figure ~~4~~ Figure 4b, 4e). Finally, Ω<sub>Ar</sub> ~~was calculated, to~~ increased from ~2.7 to ~7.8 after 2 hours, before steadily decreasing to ~6.4 on day 14 (Figure ~~4~~ Figure 4c, 4f).

~~After 10 minutes, 1 hour, 1 day, and 1 week, dilutions of the ~500 μmol kg<sup>-1</sup> of TA by Ca(OH)<sub>2</sub> addition were performed.~~ In these diluted sample treatments, ΔTA remained relatively stable over time, until the end of the experiments on day 29, regardless of dilution time (Figure ~~4~~ Figure 4a, 4d). Upon dilution, ΔTA was reduced, being very similar for the 10 minutes, 1 hour and 1 day dilutions. Overall, ΔTA in the 1 week dilution, however, ΔTA was slightly lower, i.e., ~205 μmol kg<sup>-1</sup> instead of ~230 μmol kg<sup>-1</sup> on average. In all dilutions, ΔDIC increased over time, ranging between ~20 μmol kg<sup>-1</sup> and ~60 μmol kg<sup>-1</sup>, independent of dilution timing. Finally, Ω<sub>Ar</sub> showed similar trends like ΔTA, reaching between ~4.8 and ~5.2, and slightly decreasing over time until end of the experiment.

#### 3.5.2 2000 μmol kg<sup>-1</sup> addition

~~Similarly to the previous experiment, this set of experiments consisted aimed for~~ a TA increase of ~2000 μmol kg<sup>-1</sup> by Ca(OH)<sub>2</sub> addition. However, The ~~the~~ TA only increased to ~1/3 of the theoretical value~~alkalinity addition~~, i.e., ~725 μmol kg<sup>-1</sup> within the first two hours (~~a,~~ Figure 4d). Following this increase, TA rapidly decreased during the first day, reaching a ΔTA of about -1260 μmol kg<sup>-1</sup>, and -1440 μmol kg<sup>-1</sup> in the following week (~~a,~~ Figure 4d). Over the second week of the experiment ~~From then on~~, TA appeared to stabilise up to day 14, before slightly increasing until day 21. ~~A similar trend was observed for~~ In contrast, ΔDIC, decreasing ~~decreased~~ by ~580 μmol kg<sup>-1</sup> already within the first two hours, before radically rapidly dropping to about -1590 μmol kg<sup>-1</sup> on day 1, and -1660 μmol kg<sup>-1</sup> after 7 days (~~b,~~ Figure 4e). Over the remaining 41

days,  $\Delta$ DIC then increased by  $\sim 210 \mu\text{mol kg}^{-1}$ , although remaining about  $1450 \mu\text{mol kg}^{-1}$  under the starting DIC concentration. Finally,  $\Omega_{\text{Ar}}$  reached up increased to  $\sim 16.7$  after 2 hours of reaction, followed by a rapid drop down to  $\sim 3.2$  on day 1 and  $\sim 2.0$  on day 14, while slightly increasing the following 34 days, varying between 2.0 and 2.1 (e, 4Figure 4f).

~~Dilutions were performed after 10 minutes, 1 hour, 1 day and 1 week after  $\text{Ca}(\text{OH})_2$  addition, in this case in a 1:7 ratio.~~ Concerning  $\Delta$ TA,  $\Delta$ DIC and  $\Omega_{\text{Ar}}$ , the 10 minutes and 1 hour dilutions showed similar responses, as did the 1 day and 1 week dilutions. Upon dilution,  $\Delta$ TA reached values of  $\sim 240 \mu\text{mol kg}^{-1}$  after the 10 minutes and 1 hour dilutions, and about -160 to -190  $\mu\text{mol kg}^{-1}$  for the 1 day and 1 week dilutions. With the exception of one data point in the 1 week dilution time data,  $\Delta$ TA remained relatively constant throughout all dilution experiments (a, 4Figure 4d). DIC changes were similar to the TA changes, slowly increasing over time between  $0.6$  and  $2.5 \mu\text{mol kg}^{-1}$  per day on average, with very similar values reached for the 10 minutes and 1 hour dilutions, as opposed to the 1 day and 1 week ones (b, 4Figure 4e). In all dilutions,  $\Delta$ DIC slowly increased over time. Finally,  $\Omega_{\text{Ar}}$  dropped to from  $\sim 5.0$ - $5.1$  to  $\sim 4.0$ - $4.1$  over time in the 10 minutes and 1 hour dilutions, while it decreased from dropped to  $\sim 2.3$ - $2.8$  (~~1:7~~) to  $\sim 2.1$ - $2.2$  until day 21 in the 1 day and 1 week dilution, before increasing to  $\sim 2.6$ - $3.4$  toward the end of the experiments. In all experiments,  $\Omega_{\text{Ar}}$  decreased slightly over time after dilutions (c, 4Figure 4f).

### 3.6 Particulate inorganic carbon

With the exception of the  $\sim 1050$  TA addition by  $\text{Na}_2\text{CO}_3$  plus quartz particles, measured PIC in experiments was always higher than estimates from measured  $\Delta$ TA (Table 2Table 2). Furthermore, PIC estimated from the theoretically maximum TA increase upon full mineral dissolution,  $\Delta\text{TA}_{\text{Theo}}$ , was always higher than estimated PIC from  $\Delta$ TA, by about 7 to 14% 30% in the  $\sim 500 \mu\text{mol kg}^{-1}$  TA additions with  $\text{Ca}(\text{OH})_2$  and  $\text{CaO}$ , respectively, and up to almost 67% 90% in the experiment with  $\sim 2000 \mu\text{mol kg}^{-1}$  TA additions.

## 4 Discussion

This study presents the first results on the dissolution of  $\text{CaO}$  and  $\text{Ca}(\text{OH})_2$  in natural seawater in the context of ocean alkalinity enhancement. In some of our experiments with at least  $500 \mu\text{mol kg}^{-1}$  TA increase, secondary precipitation was detected via TA and DIC decreases, as well as PIC increases. More specifically, at TA additions leading to an  $\Omega_{\text{Ar}}$  higher than 7 (in the +500 and +1000  $\mu\text{mol kg}^{-1}$  TA treatments), we observed “runaway  $\text{CaCO}_3$  precipitation” at TA additions equal or higher than  $500 \mu\text{mol kg}^{-1}$ , i.e., not only was the added TA completely removed, but significant portions of residual seawater TA as well, until a new steady state was reached. This would vastly reduce the desired  $\text{CO}_2$  removal potential by OAE and should therefore be avoided. Hence, in a subsequent set of experiments, we simulated ocean mixing to test the required timescales to avoid and/or stop secondary  $\text{CaCO}_3$  precipitation for applications that initially have TA additions above the critical threshold.

#### 4.1 Identifying CaCO<sub>3</sub> precipitation, ~~and the problem of not un~~measured precipitation, ~~and CO<sub>2</sub> gas exchange~~

CaCO<sub>3</sub> precipitation can occur via three pathways, i.e., heterogeneous, homogeneous and pseudo-homogeneous nucleation and precipitation (Chen et al., 2005; Marion et al., 2009; Wolf et al., 2008). Heterogeneous precipitation relies on the presence of existing solid mineral phases. This differs from homogeneous precipitation, characterised by the formation of CaCO<sub>3</sub> crystals from Ca<sup>2+</sup> and CO<sub>3</sub><sup>2-</sup> ions ~~present in the solution~~ in the absence of any nucleation surfaces (Chen et al., 2005; Wolf et al., 2008). Finally, the last type of precipitation, termed pseudo-homogeneous, is similar to homogeneous nucleation, however it occurs on nuclei other than solid minerals such as colloids, organic particles or glassware in a laboratory setting (Marion et al., 2009). Concerning the  $\Omega_{\text{CaCO}_3}$  thresholds ~~beyond above~~ which CaCO<sub>3</sub> precipitation is expected to occur, the lowest would be for heterogeneous and the highest for homogeneous, with pseudo-homogeneous nucleation in between. This is because nucleation sites effectively lower the activation energy required for CaCO<sub>3</sub> precipitation (Morse et al., 2007).

When 1 mole of CaCO<sub>3</sub> is precipitated, the TA of the solution decreases by 2 moles because of the removal of 1 mole of CO<sub>3</sub><sup>2-</sup> ions, accounting which accounts for 2 moles of TA (Zeebe and Wolf-Gladrow, 2001) ~~(Equation)~~. Simultaneously, the loss of 1 mole of CO<sub>3</sub><sup>2-</sup> ions decrease the DIC concentration by 1 mole. Hence, any loss of TA and DIC following a 2:1 ratio can be linked to CaCO<sub>3</sub> precipitation (Zeebe and Wolf-Gladrow, 2001). Additionally, When when CaCO<sub>3</sub> precipitation was suspected in our experiments, SEM and particulate inorganic carbon samples were taken to confirm the presence of CaCO<sub>3</sub> and to identify which morphotypes were predominant. In the +250  $\mu\text{mol kg}^{-1}$  TA additions by CaO and Ca(OH)<sub>2</sub>, both appeared to fully dissolve without inducing CaCO<sub>3</sub> precipitation, as TA and  $\Omega_{\text{Ar}}$  quickly increased within minutes, similarly to what has been described in the literature (Chave and Suess, 1970; Rushdi et al., 1992), until reaching their respective maximum after about a day and remaining stable over weeks (Figure 1Figure 1a and 1c, Figure 2Figure 2a and 2c). A slight increase in DIC was observed over time, expected when atmospheric CO<sub>2</sub> is ingassing from the bottle headspace, which was created by removing between 150 and 200 mL each sampling point. ~~This in turn lead to slowly decreasing  $\Omega_{\text{CaCO}_3}$  at constant TA, when increasing DIC and [CO<sub>2</sub>], lowering the pH and [CO<sub>3</sub><sup>2-</sup>]~~ (Equation). The ~~reason why the~~ measured TA increase was slightly below the theoretically expected one increase, which was most likely due to a combination of impurities present (in the case of CaO, a significant fraction could be hydrated), and any loss of the finely ground material during the weighing and sieving process ~~despite all efforts~~. On average, ~~~25-2723%~~ of alkalinity added was not ~~measured-detected~~ in the experiments with CaO, and about ~~13-174%~~ in the experiments with Ca(OH)<sub>2</sub> (Table 1Table 1, Figure 1Figure 1 and Figure 2Figure 2).

In contrast, in the +500  $\mu\text{mol kg}^{-1}$  TA additions by CaO and Ca(OH)<sub>2</sub> ~~additions~~, TA started decreasing after about a day 4 hours, upon the initial increase. ~~This decrease in TA was accompanied by a decrease in DIC. In the CaO experiment (exactly the same conclusions could be reached for the Ca(OH)<sub>2</sub> experiment), TA reached a maximum of about +410  $\mu\text{mol kg}^{-1}$  after 4 hours of reaction, before dropping to about -560  $\mu\text{mol kg}^{-1}$  after 34 days, constituting an overall loss of about -970  $\mu\text{mol kg}^{-1}$ . If this TA loss would be was by CaCO<sub>3</sub> precipitation, DIC should be reduced by half this amount, i.e., about -485  $\mu\text{mol kg}^{-1}$ . And indeed, measured DIC loss was~~ very close to this 2:1 ratio in both the CaO and Ca(OH)<sub>2</sub> experiments with a TA addition

of 500  $\mu\text{mol kg}^{-1}$  (950:465 and 860:395 for CaO and Ca(OH)<sub>2</sub>, respectively) exactly the same. This suggests that TA was precipitated in the form of CaCO<sub>3</sub>. ~~Although a perfect match, a caveat here is~~ The slight off-set can be explained by ~~that the DIC loss is underestimated as of concurrent~~ ingassing of CO<sub>2</sub> from the head space which would lower the TA:DIC ratio, becoming visible when precipitation ceases towards the end (Figure 1 ~~Figure 1b~~). Hence, ~~the DIC loss should have been higher~~ Another caveat is, ~~requiring also higher TA removal than actually measured.~~ This discrepancy can be explained by the fact that the maximum increase in TA from full dissolution of CaO or Ca(OH)<sub>2</sub> cannot be measured in the presence of concurrent CaCO<sub>3</sub> precipitation. This is mostly evident in the +2000  $\mu\text{mol kg}^{-1}$  TA addition (Figure 4 ~~Figure 4~~), where DIC decreases due to CaCO<sub>3</sub> precipitation, yet TA increases due to higher Ca(OH)<sub>2</sub> dissolution rates. It also explains why estimated PIC calculated from measured TA changes ~~are is generally~~ smaller than actually measured PIC concentrations (Table 2 ~~Table 2~~). In the experiment with 1M Na<sub>2</sub>CO<sub>3</sub> and quartz particles, ~~both the measured TA-based estimated PIC estimates PIC have similar results. However,~~ were larger than the measured PIC ~~is about twice as low.~~ This ~~is difficult to explain,~~ although we ~~observed a white layer on the bottle walls, indicative of CaCO<sub>3</sub> precipitation. However, this was also observed during the other experiments with CaCO<sub>3</sub> precipitation, yet measured PIC concentrations were larger than when estimated from the TA decrease, could be explained by a combination of precipitation on both the quartz particles and bottle walls. In this sense, trying to estimate CaCO<sub>3</sub> precipitation from measured changes in TA, without considering theoretical TA generation by dissolution or actual PIC measurements, might underestimate total precipitation. Finally, next to impurities and issues with mineral handling, the reason why measured seawater PIC concentrations are in between the other estimates lies in the fact that a small portion of the CaCO<sub>3</sub> precipitated on the bottle walls, at least in the 2000  $\mu\text{mol kg}^{-1}$  TA experiment. In any case, while being a laboratory artefact, this has no practical consequences as in a natural setting, the TA would eventually precipitate in the water column. In this sense~~ summary, trying to estimate CaCO<sub>3</sub> precipitation from measured changes in TA, without knowing how much considering theoretical TA was actually generated generation by full mineral dissolution or actual PIC measurements, might underestimate total precipitation.

#### 4.2 The presence of mineral phases ~~enhances~~ triggers “runaway CaCO<sub>3</sub> precipitation”

An ~~interesting~~ important finding in our experiments was that whenever CaCO<sub>3</sub> precipitation was observed, it continued even if the solution dropped below an  $\Omega_{\text{Ar}}$  of ~4-5, levels at which no precipitation was observed in the +250  $\mu\text{mol kg}^{-1}$  TA addition experiments. We termed this phenomenon “runaway precipitation”. Furthermore, in all these experiments, precipitation decreased and seemingly ceased at a  $\Omega_{\text{Ar}}$  of ~1.8-2.0. It therefore appears that when CaCO<sub>3</sub> is initially precipitated, CaCO<sub>3</sub> continues to precipitate in a runaway fashion, even if  $\Omega_{\text{Ar}}$  drops below levels where precipitation would not be initiated in natural seawater. This is to be expected as ~~precipitation rates of CaCO<sub>3</sub> into precipitates onto~~ CaCO<sub>3</sub> mineral phases at any saturation state above 1, and the initial precipitation at high saturation states provides new nucleation sites. (Morse et al., 2007; Morse et al., 2003; Zhong and Mucci, 1989). ~~The precipitation rate is are~~ directly related-proportional to  $\Omega_{\text{CaCO}_3}$ , decreasing exponentially until reaching zero at an  $\Omega_{\text{CaCO}_3}$  value of 1 (Figure A 4)-. However, the question of why did

precipitation occurred at a much lower  $\Omega_{\text{CaCO}_3}$ , i.e.  $\Omega_{\text{Ar}} \sim 7.5$ , than ~~expected/anticipated~~, (i.e.,  $\Omega_{\text{CaCO}_3} \sim 7.5$  vs  $\sim 12.3$ ) remains (Marion et al., 2009)?.

It is known that the presence of particles in suspension can initiate and accelerate  $\text{CaCO}_3$  precipitation (Millero et al., 2001; Morse et al., 2003; Wurgaft et al., 2021). It is unlikely that the presence of  $\text{CaCO}_3$  impurities in  $\text{CaO}$  (less than 1% carbon) and  $\text{Ca(OH)}_2$  (less than 2% carbon) from imperfect calcination would have caused precipitation, as the presence of  $\text{CaCO}_3$  mineral phases should have caused precipitation at any saturation state above 1, i.e., also in the  $+250 \mu\text{mol kg}^{-1}$  TA addition experiments. Furthermore, modelling precipitation using experimentally determined  $\Omega_{\text{Ar}}$  and surface area dependant aragonite precipitation rates onto  $\text{CaCO}_3$  mineral phases ~~Zhong and Mucci (1989)~~ (Zhong and Mucci, 1989), suggests that once precipitation becomes analytically detectable, it should proceed very rapidly before levelling off, i.e., ~~within a couple of days (Figure A 5)~~. Furthermore, while we expected  $\text{CaCO}_3$  precipitation to stop at an  $\Omega_{\text{Ar}} \sim 1$ , we observed it to stop at  $\Omega_{\text{Ar}}$  of  $\sim 2$ . However, that is in contrast to what we observed here. The presence of dissolved organic carbon could have been slowing down if not stopping  $\text{CaCO}_3$  precipitation at an  $\Omega_{\text{Ar}}$  higher than 1 (Chave and Suess, 1970; Pan et al., 2021). We also observed that the bulk of precipitation ~~occurring~~ occurred over a period of at least a week, after which an equilibration was reached with apparent differences between the different dissolving minerals (i.e.,  $\text{CaO}$ ,  $\text{Ca(OH)}_2$  and quartz, although it is acknowledged that the experiments were not replicated).

Another explanation for  $\text{CaCO}_3$  precipitation is heterogeneous precipitation on not yet dissolved  $\text{CaO}$  and  $\text{Ca(OH)}_2$  particles (or other impurities), leading to  $\text{CaCO}_3$  crystal formation and initiating runaway precipitation. The  $\Omega_{\text{Ar}}$  threshold for this process would depend on lattice compatibility of the mineral phases (Tang et al., 2020). For instance,  $\text{CaCO}_3$  precipitation has been observed at any saturation states above 1 when introducing  $\text{CaCO}_3$  seed particles. In contrast, Lioliou et al. (2007) ~~did not report  $\text{CaCO}_3$  precipitation onto quartz particles at the addition of quartz particles did not trigger precipitation at an  $\Omega_{\text{Ar}}$  of up to lower than 3.5~~. For that to occur and in order to trigger  $\text{CaCO}_3$  precipitation onto quartz particles,  $\Omega_{\text{Ar}}$  would need to be further increased. And Here, we indeed, observed  $\text{CaCO}_3$  precipitation above at an  $\Omega_{\text{Ar}}$  of  $\sim 9.2$ ,  $\text{CaCO}_3$  precipitation did actually occur (Figure 3). The reason for an initially slower but then more rapid precipitation could be a combination of exponentially increasing  $\text{CaCO}_3$  surface area, as well as concomitantly increasing lattice compatibility (Lioliou et al., 2007; Pan et al., 2021). The filtration of TA enriched seawater supports this idea. ~~Not, since not~~ yet dissolved mineral phases that could facilitate early nucleation are removed, preventing runaway  $\text{CaCO}_3$  precipitation (Figure 3).

Needle-shaped aragonite precipitation onto quartz particles (Figure 5c and 5d) was directly observed by SEM imaging, ~~and confirmed by EDX analysis/analyses, identifying/identified~~ the larger ~~base~~ mineral to be rich in silicon, a key characteristic of quartz, and the needle-shaped particles composed of carbon, oxygen and calcium, indicative for  $\text{CaCO}_3$  (Chang et al., 2017; Ni and Ratner, 2008; Pan et al., 2021). In contrast, direct aragonite precipitation onto not yet dissolved  $\text{CaO}$  and  $\text{Ca(OH)}_2$  in the  $+500 \mu\text{mol kg}^{-1}$  TA addition is difficult to prove as EDX analyses revealed the presence of Ca and O, both present in the mineral feedstocks and aragonite by  $\text{CaO}$  and  $\text{Ca(OH)}_2$  did not reveal any insoluble base element other than Ca, suggesting initial  $\text{CaCO}_3$  precipitation onto  $\text{CaO}$  and  $\text{Ca(OH)}_2$  (Figure 5a and 5b). In Finally, in some situations (Figure 5b), round crystals were also observed, suggesting the presence of vaterite (Chang et al., 2017).

However, aragonite crystals represented the majority of  $\text{CaCO}_3$  observed by SEM. ~~Early  $\text{CaCO}_3$  precipitation onto  $\text{CaO}$  and  $\text{Ca}(\text{OH})_2$  particles, providing some sort of coating could also, or at least partially, explain why maximum measured TA was lower than theoretically anticipated.~~

### 4.3 Impacts of $\text{CaCO}_3$ precipitation on OAE potential

475 From an OAE perspective,  $\text{CaCO}_3$  precipitation is an important chemical reaction that needs to be avoided. ~~When  $\text{CaCO}_3$  precipitates, TA and DIC decrease in a 2:1 fashion. During  $\text{CaCO}_3$  precipitation, Simultaneously,~~ dissolved  $[\text{CO}_3^{2-}]$  and  $\Omega_{\text{CaCO}_3}$  are decreasing, and  $[\text{CO}_2]$  is increasing, ~~which reduces the ocean's uptake capacity for atmospheric  $\text{CO}_2$ , hence~~ impacting OAE potential. Considering typical open ocean TA and DIC concentrations of 2350 and 2100  $\mu\text{mol kg}^{-1}$  respectively, at a salinity of 35 and a temperature of 19 °C, this water mass would have a  $\text{pCO}_2$  close to atmospheric equilibrium  
480 ~~of, ~416  $\mu\text{atmppm}$ , a  $\text{pH}_T$  value (total scale) of ~8.04, and an  $\Omega_{\text{Ar}}$  of ~2.80. Without  $\text{CaCO}_3$  precipitation, an addition of 500  $\mu\text{mol kg}^{-1}$  TA would lower  $\text{pCO}_2$  to ~92  $\mu\text{atm}$  and increase  $\text{pH}_T$  and  $\Omega_{\text{Ar}}$  to about 8.61 and 8.45 respectively. If fully re-~~  
485 ~~equilibrated with the atmosphere, DIC would increase by about 420  $\mu\text{mol kg}^{-1}$ , leading to a  $\text{pH}_T$  and  $\Omega_{\text{Ar}}$  0.07 and 1.10 higher than prior to the addition, respectively (Table 3Table 3). The resulting OAE efficiency would be 0.83 mole of atmospheric  $\text{CO}_2$  absorbed per mole of TA, very similar to estimates by Köhler et al. (2010). Considering that  $\text{CaCO}_3$  is the base-source~~  
490 ~~material for  $\text{CaO}$  and  $\text{Ca}(\text{OH})_2$ , and the fact that 2 moles of TA are produced per mole of mineral dissolution, ~0.7 tonnes of  $\text{CO}_2$  could be captured per tonne of source material, assuming  $\text{CO}_2$  capture during the calcination process. At a global-scale, using all available ship capacity and assuming a slow discharge of 1.7 to 4.0 Gt of  $\text{Ca}(\text{OH})_2$  per year (Caserini et al., 2021), between 1.2 and 2.8 Gt of  $\text{CO}_2$  per year could be absorbed by the ocean. Including direct coastal TA discharge at Similarly,~~  
495 ~~following the models from with a constant addition of  $\text{Ca}(\text{OH})_2$  at 10  $\text{Gt}\cdot\text{year}^{-1}$  (Feng et al., 2016), we could expect to absorb about an additional 7 Gt of  $\text{CO}_2$  per year. This would eventually lead to more than 546 Gt of  $\text{CO}_2$  by 2100 if implemented in 2022. To put these model-derived numbers into perspective, the global cement industry currently produces about 4.1 Gt of cement per year (Statista, 2021). Depending on whether hydraulic ( $4\text{CaO}\cdot\text{Al}_2\text{O}_3\cdot\text{Fe}_2\text{O}_3$ ) or non-hydraulic ( $\text{Ca}(\text{OH})_2$ ) cement is being produced, and assuming a molar  $\text{Ca}^{2+}$  to  $\text{CO}_2$  sequestration potential of 1.6, up to 3.9 Gt of atmospheric  $\text{CO}_2$  could be captured per year. This is on the order required to be built-up in the next 30 years, based on the shared socioeconomic pathways RCP2.6 scenario that would keep global warming below the 2 °C target (Huppmann et al., 2018).~~

495 However, these ~~substantial~~ numbers ~~can only be obtained when dissolution is assume a complete dissolution~~ without  $\text{CaCO}_3$  precipitation. ~~Hypothetically, if~~ as much  $\text{CaCO}_3$  precipitates as TA was added, only ~~0.50-1~~ instead of 1.6 mole of DIC can be absorbed per 2 moles of TA after equilibration with atmospheric  $\text{pCO}_2$  (Table 3Table 3). This represent a decrease by nearly 40% in OAE potential. Similarly, ~~assuming~~ runaway  $\text{CaCO}_3$  precipitation until ~~an  $\Omega_{\text{Ar}}$  = of 2.0, as observed here,~~  
500 ~~decreases the OAE potential further by almost 90%. Then, only ~0.11 mole of DIC would be absorbed per mole of TA added (Table 3Table 3). Finally~~ Furthermore, secondary  $\text{CaCO}_3$  precipitation higher than TA addition will lead to  $\text{pH}_T$  and  $\Omega_{\text{CaCO}_3}$  levels lower than initial ones. For instance, runaway precipitation for a TA addition of 500  $\mu\text{mol kg}^{-1}$  will see  $\text{pH}_T$  drop by about 0.1 from 8.04 to 7.93 and  $\Omega_{\text{Ar}}$  from 2.80 to 1.66, significantly enhancing ongoing ocean acidification (Table 3Table 3).



Runaway CaCO<sub>3</sub> precipitation for a TA addition of 1000 μmol kg<sup>-1</sup> (~~assumed to cease at an Ω<sub>Ar</sub> of 2 as observed here~~) would even see Ω<sub>Ar</sub> drop ~~further, i.e., to~~ below 1, ~~upon CO<sub>2</sub> re-equilibration with the atmosphere (Table 3)~~. Under such conditions, aragonite ~~would start to dissolve, impacting various living beings, as it is~~ an important biomineral for a variety of marine organisms, e.g., sessile corals, benthic molluscs and planktonic pteropods, ~~would start to dissolve~~ (Riebesell et al., 2011; Zeebe and Wolf-Gladrow, 2001). In summary, runaway CaCO<sub>3</sub> precipitation in OAE has to be avoided as not only reducing CO<sub>2</sub> uptake efficiency significantly but also capable of enhancing ocean acidification. Keeping track of OAE efficiency from changes in TA concentrations can be challenging as CaCO<sub>3</sub> precipitation can be underestimated as described earlier, requiring new and clever monitoring strategies ~~to ensure effective dilutions take place~~.

#### 4.4 Avoiding CaCO<sub>3</sub> precipitation by dilution and other TA addition strategies

~~While above considerations stress the importance for monitoring~~ An important aspect when it comes to avoiding CaCO<sub>3</sub> precipitation, ~~they do not take into account the natural~~ is the dilution that would occur in the wake of ships releasing TA in the ocean, or by natural mixing of TA-enriched water with surrounding seawater (Caserini et al., 2021; Feng et al., 2017; Mongin et al., 2021). In our experiments, a 1:1 dilution ~~could seemingly stop of seawater in which~~ CaCO<sub>3</sub> precipitation in seawater, was taking place upon a 500 μmol kg<sup>-1</sup> TA addition was seemingly stopped, even if ~~initiated~~ performed only after one week for the +500 μmol kg<sup>-1</sup> TA addition. ~~This~~ At a first glance, this comes ~~a bit~~ at a surprise as precipitation nuclei would only be diluted by half, hence reducing surface area and precipitation rates by a factor of 2. However, as Ω<sub>Ar</sub> is significantly reduced simultaneously, precipitation rates are further reduced by a factor of 10 (see ~~Figure A 4~~ Figure A-4). Hence, overall precipitation would see a reduction by a factor of 20. This ~~however~~, should slow down continuing precipitation initially, if on CaCO<sub>3</sub> particles, but not completely inhibit it (Zhong and Mucci, 1989). A possible explanation could be that dilution would have lowered Ω<sub>Ar</sub> below the critical threshold for overcoming lattice mismatch, as most of the aragonite precipitation appears to be on the original seed mineral itself rather than on the newly formed aragonite (compare ~~Figure 5~~ Figure 5c and 5d).

Overall, CaCO<sub>3</sub> precipitation ~~can~~ could be avoided if the TA+500 μmol kg<sup>-1</sup> enriched ~~sample seawater~~ is diluted 1:1, reaching an Ω<sub>Ar</sub> of ~5.0. The quicker dilution takes place, the less CaCO<sub>3</sub> would precipitate prior. Similar results were found for a TA addition of +2000 μmol kg<sup>-1</sup>, i.e., the ability to stop precipitation at an Ω<sub>Ar</sub> of ~5.0, after a 1:7 dilution. However, only the 10 minutes and 1 hour dilutions seem to be suitable in an OAE context, as much more rapidly occurring aragonite precipitation at a higher initial Ω<sub>Ar</sub> of about 16.7 would significantly reduce the CO<sub>2</sub> uptake efficiency. Furthermore, the difficulty to monitor precipitation ~~form from~~ simple TA measurements (as described above) would also mean that ~~verification of permanent quantification of~~ CO<sub>2</sub> removal is ~~problematic~~ not straight-forward. Hence, in order to assign carbon credits, TA additions have to be done in a way that rule out or at least minimise secondary CaCO<sub>3</sub> precipitation. This is ~~the case~~ true for any type of TA addition, and is not specific to quick and hydrated lime.

Adding TA from land, as modelled by Feng et al. (2017), shows that the more TA is added, the higher coastal Ω<sub>Ar</sub> would be. ~~Staying~~ By staying clearly below the Ω<sub>Ar</sub> ~~5~~ threshold ~~identified here, i.e., limiting coastal Ω<sub>Ar</sub> to only 3.2~~, up to ~550 Gt of carbon in the form of CO<sub>2</sub> could be removed from the atmosphere by 2100, corresponding to a reduction ~~of by~~ about 260 ppm

(Feng et al., 2017). The critical  $\Omega_{Ar}$  threshold beyond which secondary  $\text{CaCO}_3$  precipitation would be observed could be higher for other minerals, theoretically allowing for higher TA additions. However, it has to be kept in mind that in waters with high sediment load, often found in coastal settings,  $\text{CaCO}_3$  could precipitate onto other mineral particles than those added to increase TA. This has been observed in river plumes (Wurgaft et al., 2021), on the Bahama Banks by resuspended sediments (Bustos-Serrano et al., 2009) and in the Red Sea following flash flood deposition of resuspended sediments and particles (Wurgaft et al., 2016). Hence, even with minerals potentially allowing for higher TA additions, an  $\Omega_{Ar}$  threshold of 5 might be safer to adopt. However, atmospheric  $\text{CO}_2$  removal could be increased if TA would also be added to the open ocean, e.g., on ships of opportunity. Here, additions could be much higher as ship movement and rapid mixing within its wake would significantly dilute added TA (Caserini et al., 2021; Köhler et al., 2013) as opposed to coastal point sources.

Finally, another option to increase atmospheric  $\text{CO}_2$  uptake would be to ~~not add minerals to seawater directly, not add mineral to seawater directly,~~ but to keep the seawater first-equilibrated it-with air or  $\text{CO}_2$  enriched flumes/flue gases, during mineral dissolution to atmospheric  $\text{pCO}_2$  levels while dissolving. This-Firstly, this would allow reaching an  $\Omega_{Ar}$  of 5 when equilibrated with the atmosphere, as opposed to 3.3 in the +250  $\mu\text{mol kg}^{-1}$  TA scenario (Table 3), when equilibration is slow and passive, after +250  $\mu\text{mol kg}^{-1}$  TA increase (-) occurs after instead of during the dissolution process. And secondly, when reaching an  $\Omega_{Ar}$  of 5 with  $\text{CO}_2$  equilibration, In this case, nearly 1000 instead of 250  $\mu\text{mol kg}^{-1}$  of TA could be added, allowing for almost 4 times the amount of atmospheric  $\text{CO}_2$  to be removed (this number is highly sensitive to temperature, and ranges between ~3 and ~6 between 30 and 5 °C). However, this represent an extra step, which appears to be far more time and cost consuming than a simple mineral addition. It has also to be kept in mind that for the same  $\Omega_{Ar}$  threshold, the amount of TA that can be added will increase with lower temperature, as of higher  $\text{CO}_2$  solubility and hence naturally lower  $\Omega_{Ar}$  in colder waters. Based on our  $\Omega_{Ar}$  threshold of 5, At a salinity of 35 and at 5 °C, about three times as much TA can be dissolved as opposed to a temperature of 30 °C.

## 5 Conclusions

Ocean alkalinity enhancement is a ~~promising~~-negative emission technology with relatively large potential for atmospheric  $\text{CO}_2$  removal (Caserini et al., 2021; Feng et al., 2016; Köhler et al., 2010). In order to maximise carbon dioxide ( $\text{CO}_2$ ) uptake efficiency, secondary calcium carbonate ( $\text{CaCO}_3$ ) precipitation has to be avoided. Here, we show that an increase of total alkalinity (TA) by 500  $\mu\text{mol kg}^{-1}$  led to aragonite precipitation, reducing the  $\text{CO}_2$  uptake potential from about 0.8 moles per mole of alkalinity added to less than 0.2 moles. Precipitation ~~was~~-most likely occurred onto the  $\text{CaO}$  and  $\text{Ca}(\text{OH})_2$  mineral phases prior to their full dissolution. In contrast, an addition of 250  $\mu\text{mol kg}^{-1}$  of TA did not result in  $\text{CaCO}_3$  precipitation, suggesting that an aragonite saturation state ( $\Omega_{Ar}$ ) of about 5 is a safe ~~upper~~-limit. This is probably also the case for other minerals ~~that with even lower lattice compatibility for  $\text{CaCO}_3$ , because in coastal settings,  $\text{CaCO}_3$  could precipitate would theoretically allow for higher TA additions as of potential precipitation~~ onto naturally present mineral phases, such as resuspended sediments ~~in coastal settings~~. Safely increasing the amount of TA that could be added to the ocean involves could

570 ~~be achieved by expanding to the open ocean by ships of opportunity,~~ allowing for major mixing and dilution of enriched seawater by coastal tides or in the wake of ships, equilibrating the seawater to atmospheric CO<sub>2</sub> levels prior to the addition during mineral dissolution, and/or targeting low rather than high temperature ~~regimes~~regions.

### **Data availability**

Data will be made available on a publicly available repository upon final publication.

### **Author contributions**

575 CAM and KGS designed the initial experiments. All co-authors contributed to the initial data analysis and designing of follow-up experiments. CAM performed most of the sampling, and the data analyses with the help of KGS. CAM wrote the paper with KGS, with inputs from their respective fields of expertise by all co-authors.

### **Competing interests**

The authors declare that they have no conflict of interest.

### 580 **Acknowledgements**

We would like to thank Marian Bailey for her help with ICPMS sample preparation, as well as Dr Nick Ward for his help with preliminary X-ray Diffraction analyses of the calcium powders. We are also thankful to Dr Matheus Carvalho de Carvalho for the particulate carbon analyses and Nadia Toppler for her help arranging the use of the SEM.

### **Financial support**

585 This research is part of the PhD project of CAM that is funded by a Cat. 5 – SCU Grad School scholarship from the Southern Cross University, Lismore, Australia. The ICPMS analyses were made possible by the Australian Research Council grants number LE200100022 by RJB and KGS, and LE120100201 obtained by RJB.

590 **References**

- Bach, L. T., Gill, S., Rickaby, R., Gore, S., and Renforth, P.: CO<sub>2</sub> removal with enhanced weathering and ocean alkalinity enhancement: Potential risks and co-benefits for marine pelagic ecosystems, *Frontiers in Climate*, 1, 7, 2019.
- Bates, N., Best, M., Neely, K., Garley, R., Dickson, A., and Johnson, R.: Detecting anthropogenic carbon dioxide uptake and ocean acidification in the North Atlantic Ocean, *Biogeosciences Discussions*, 9, 2012.
- 595 Berner, R.: The role of magnesium in the crystal growth of calcite and aragonite from sea water, *Geochimica et Cosmochimica Acta*, 39, 489-504, 1975.
- Boyd, P., Vivian, C., Boettcher, M., Chai, F., Cullen, J., Goeschl, T., Lampitt, R., Lenton, A., Oschlies, A., and Rau, G.: High level review of a wide range of proposed marine geoengineering techniques, 2019.
- 600 Burt, D. J., Fröb, F., and Ilyina, T.: The sensitivity of the marine carbonate system to regional ocean alkalinity enhancement, *Frontiers in Climate*, 3, 2021.
- Bustos-Serrano, H., Morse, J. W., and Millero, F. J.: The formation of whittings on the Little Bahama Bank, *Marine Chemistry*, 113, 1-8, 2009.
- Canadell, J. G., Le Quéré, C., Raupach, M. R., Field, C. B., Buitenhuis, E. T., Ciais, P., Conway, T. J., Gillett, N. P., Houghton, R., and Marland, G.: Contributions to accelerating atmospheric CO<sub>2</sub> growth from economic activity, carbon intensity, and efficiency of natural sinks, *Proceedings of the national academy of sciences*, 104, 18866-18870, 2007.
- 605 Carter, B. R., Feely, R. A., Wanninkhof, R., Kouketsu, S., Sonnerup, R. E., Pardo, P. C., Sabine, C. L., Johnson, G. C., Sloyan, B. M., and Murata, A.: Pacific anthropogenic carbon between 1991 and 2017, *Global Biogeochemical Cycles*, 33, 597-617, 2019.
- Caserini, S., Pagano, D., Campo, F., Abbà, A., De Marco, S., Righi, D., Renforth, P., and Grosso, M.: Potential of Maritime Transport for Ocean Liming and Atmospheric CO<sub>2</sub> Removal, *Frontiers in Climate*, 3, 22, 2021.
- 610 Chang, R., Kim, S., Lee, S., Choi, S., Kim, M., and Park, Y.: Calcium carbonate precipitation for CO<sub>2</sub> storage and utilization: a review of the carbonate crystallization and polymorphism, *Frontiers in Energy Research*, 5, 17, 2017.
- Chave, K. E. and Suess, E.: Calcium Carbonate Saturation in Seawater: Effects of Dissolved Organic Matter 1, *Limnology and Oceanography*, 15, 633-637, 1970.
- Chen, T., Neville, A., and Yuan, M.: Calcium carbonate scale formation—assessing the initial stages of precipitation and deposition, *Journal of Petroleum Science and Engineering*, 46, 185-194, 2005.
- 615 Cyronak, T., Schulz, K. G., Santos, I. R., and Eyre, B. D.: Enhanced acidification of global coral reefs driven by regional biogeochemical feedbacks, *Geophysical Research Letters*, 41, 5538-5546, 2014.
- De Choudens-Sanchez, V. and Gonzalez, L. A.: Calcite and aragonite precipitation under controlled instantaneous supersaturation: elucidating the role of CaCO<sub>3</sub> saturation state and Mg/Ca ratio on calcium carbonate polymorphism, *Journal of Sedimentary Research*, 79, 363-376, 2009.
- 620 Dickson, A. and Millero, F. J.: A comparison of the equilibrium constants for the dissociation of carbonic acid in seawater media, *Deep Sea Research Part A. Oceanographic Research Papers*, 34, 1733-1743, 1987.
- Dickson, A. G.: Standards for ocean measurements, *Oceanography*, 23, 34-47, 2010.
- Dickson, A. G., Sabine, C. L., and Christian, J. R.: Guide to best practices for ocean CO<sub>2</sub> measurements, *North Pacific Marine Science Organization*2007.
- 625 Doney, S. C., Fabry, V. J., Feely, R. A., and Kleypas, J. A.: Ocean acidification: the other CO<sub>2</sub> problem, *Annual review of marine science*, 1, 169-192, 2009.
- Feng, E., Koeve, W., Keller, D. P., and Oschlies, A.: Model-Based Assessment of the CO<sub>2</sub> Sequestration Potential of Coastal Ocean Alkalinization, *Earth's Future*, 5, 1252-1266, 2017.
- Feng, E. Y., Keller, D. P., Koeve, W., and Oschlies, A.: Could artificial ocean alkalinization protect tropical coral ecosystems from ocean acidification?, *Environmental Research Letters*, 11, 074008, 2016.
- 630 Gafar, N. A. and Schulz, K. G.: A three-dimensional niche comparison of *Emiliana huxleyi* and *Gephyrocapsa oceanica*: reconciling observations with projections, *Biogeosciences*, 15, 3541-3560, 2018.
- Gattuso, J.-P., Magnan, A., Billé, R., Cheung, W. W., Howes, E. L., Joos, F., Allemand, D., Bopp, L., Cooley, S. R., and Eakin, C. M.: Contrasting futures for ocean and society from different anthropogenic CO<sub>2</sub> emissions scenarios, *Science*, 349, aac4722, 2015.
- 635 González, M. F. and Ilyina, T.: Impacts of artificial ocean alkalinization on the carbon cycle and climate in Earth system simulations, *Geophysical Research Letters*, 43, 6493-6502, 2016.
- Goodwin, P., Brown, S., Haigh, I. D., Nicholls, R. J., and Matter, J. M.: Adjusting mitigation pathways to stabilize climate at 1.5 C and 2.0 C rise in global temperatures to year 2300, *Earth's Future*, 6, 601-615, 2018.
- 640 Harvey, L.: Mitigating the atmospheric CO<sub>2</sub> increase and ocean acidification by adding limestone powder to upwelling regions, *Journal of Geophysical Research: Oceans*, 113, 2008.

- Hoegh-Guldberg, O., Jacob, D., Taylor, M., Bolaños, T. G., Bindi, M., Brown, S., Camilloni, I., Diedhiou, A., Djalante, R., and Ebi, K.: The human imperative of stabilizing global climate change at 1.5° C, *Science*, 365, eaaw6974, 2019.
- Hoegh-Guldberg, O., Mumby, P. J., Hooten, A. J., Steneck, R. S., Greenfield, P., Gomez, E., Harvell, C. D., Sale, P. F., Edwards, A. J., and Caldeira, K.: Coral reefs under rapid climate change and ocean acidification, *science*, 318, 1737-1742, 2007.
- 645 Huppmann, D., Kriegler, E., Krey, V., Riahi, K., Rogelj, J., Rose, S. K., Weyant, J., Bauer, N., Bertram, C., and Bosetti, V.: IAMC 1.5 C Scenario Explorer and Data hosted by IIASA, Integrated Assessment Modeling Consortium & International Institute for Applied Systems Analysis, 10, 2018.
- Ilyina, T., Wolf-Gladrow, D., Munhoven, G., and Heinze, C.: Assessing the potential of calcium-based artificial ocean alkalization to mitigate rising atmospheric CO<sub>2</sub> and ocean acidification, *Geophysical Research Letters*, 40, 5909-5914, 2013.
- 650 IPCC: Climate Change 2021: The Physical Science Basis. Contribution of Working Group I to the Sixth Assessment Report of the Intergovernmental Panel on Climate Change [Masson-Delmotte, V., P. Zhai, A. Pirani, S. L. Connors, C. Péan, S. Berger, N. Caud, Y. Chen, L. Goldfarb, M. I. Gomis, M. Huang, K. Leitzell, E. Lonnoy, J. B. R. Matthews, T. K. Maycock, T. Waterfield, O. Yelekçi, R. Yu and B. Zhou (eds.)]. Cambridge University Press. In Press., 2021.
- Keller, D. P., Feng, E. Y., and Oschlies, A.: Potential climate engineering effectiveness and side effects during a high carbon dioxide-emission scenario, *Nature communications*, 5, 1-11, 2014.
- 655 Kheshgi, H. S.: Sequestering atmospheric carbon dioxide by increasing ocean alkalinity, *Energy*, 20, 915-922, 1995.
- Köhler, P., Hartmann, J., and Wolf-Gladrow, D. A.: Geoengineering potential of artificially enhanced silicate weathering of olivine, *Proceedings of the National Academy of Sciences*, 107, 20228-20233, 2010.
- Köhler, P., Abrams, J. F., Völker, C., Hauck, J., and Wolf-Gladrow, D. A.: Geoengineering impact of open ocean dissolution of olivine on atmospheric CO<sub>2</sub>, surface ocean pH and marine biology, *Environmental Research Letters*, 8, 014009, 2013.
- 660 Lenton, A., Matear, R. J., Keller, D. P., Scott, V., and Vaughan, N. E.: Assessing carbon dioxide removal through global and regional ocean alkalization under high and low emission pathways, *Earth System Dynamics*, 9, 339-357, 2018.
- Lenton, T. and Vaughan, N.: The radiative forcing potential of different climate geoengineering options. *Atmos. Chem. Phys. Discuss.*, V, 2009.
- 665 Lewis, E. and Perkin, R.: The practical salinity scale 1978: conversion of existing data, *Deep Sea Research Part A. Oceanographic Research Papers*, 28, 307-328, 1981.
- Lioliou, M. G., Paraskeva, C. A., Koutsoukos, P. G., and Payatakes, A. C.: Heterogeneous nucleation and growth of calcium carbonate on calcite and quartz, *Journal of colloid and interface science*, 308, 421-428, 2007.
- Lueker, T. J., Dickson, A. G., and Keeling, C. D.: Ocean pCO<sub>2</sub> calculated from dissolved inorganic carbon, alkalinity, and equations for K<sub>1</sub> and K<sub>2</sub>: validation based on laboratory measurements of CO<sub>2</sub> in gas and seawater at equilibrium, *Marine chemistry*, 70, 105-119, 2000.
- 670 Marion, G., Millero, F. J., and Feistel, R.: Precipitation of solid phase calcium carbonates and their effect on application of seawater SA-T-P models, *Ocean Science*, 5, 285, 2009.
- Mehrbach, C., Culbertson, C., Hawley, J., and Pytkowicz, R.: Measurement of the apparent dissociation constants of carbonic acid in seawater at atmospheric pressure 1, *Limnology and oceanography*, 18, 897-907, 1973.
- 675 Millero, F., Huang, F., Zhu, X., Liu, X., and Zhang, J.-Z.: Adsorption and desorption of phosphate on calcite and aragonite in seawater, *Aquatic Geochemistry*, 7, 33-56, 2001.
- Mongin, M., Baird, M. E., Lenton, A., Neill, C., and Akl, J.: Reversing ocean acidification along the Great Barrier Reef using alkalinity injection, *Environmental Research Letters*, 16, 064068, 2021.
- 680 Montserrat, F., Renforth, P., Hartmann, J., Leermakers, M., Knops, P., and Meysman, F. J.: Olivine dissolution in seawater: implications for CO<sub>2</sub> sequestration through enhanced weathering in coastal environments, *Environmental science & technology*, 51, 3960-3972, 2017.
- Morse, J. W. and He, S.: Influences of T, S and PCO<sub>2</sub> on the pseudo-homogeneous precipitation of CaCO<sub>3</sub> from seawater: implications for whiting formation, *Marine Chemistry*, 41, 291-297, 1993.
- Morse, J. W., Arvidson, R. S., and Lüttge, A.: Calcium carbonate formation and dissolution, *Chemical reviews*, 107, 342-381, 2007.
- 685 Morse, J. W., Gledhill, D. K., and Millero, F. J.: CaCO<sub>3</sub> precipitation kinetics in waters from the great Bahama bank: Implications for the relationship between bank hydrochemistry and whittings, *Geochimica et Cosmochimica Acta*, 67, 2819-2826, 2003.
- Morse, J. W., Wang, Q., and Tsio, M. Y.: Influences of temperature and Mg: Ca ratio on CaCO<sub>3</sub> precipitates from seawater, *Geology*, 25, 85-87, 1997.
- Mucci, A.: The solubility of calcite and aragonite in seawater at various salinities, temperatures, and one atmosphere total pressure, *Am. J. Sci*, 283, 780-799, 1983.
- 690 National Academies of Sciences, E. and Medicine: A Research Strategy for Ocean-based Carbon Dioxide Removal and Sequestration, The National Academies Press, Washington, DC, 360 pp., doi:10.17226/26278, 2021.

Ni, M. and Ratner, B. D.: Differentiating calcium carbonate polymorphs by surface analysis techniques—an XPS and TOF-SIMS study, *Surface and Interface Analysis: An International Journal devoted to the development and application of techniques for the analysis of surfaces, interfaces and thin films*, 40, 1356-1361, 2008.

695 Pan, Y., Li, Y., Ma, Q., He, H., Wang, S., Sun, Z., Cai, W.-J., Dong, B., Di, Y., and Fu, W.: The role of Mg<sup>2+</sup> in inhibiting CaCO<sub>3</sub> precipitation from seawater, *Marine Chemistry*, 104036, 2021.

Pytkowicz, R. M.: Rates of inorganic calcium carbonate nucleation, *The Journal of Geology*, 73, 196-199, 1965.

Renforth, P. and Henderson, G.: Assessing ocean alkalinity for carbon sequestration, *Reviews of Geophysics*, 55, 636-674, 2017.

Renforth, P. and Kruger, T.: Coupling mineral carbonation and ocean liming, *Energy & fuels*, 27, 4199-4207, 2013.

700 Renforth, P., Jenkins, B., and Kruger, T.: Engineering challenges of ocean liming, *Energy*, 60, 442-452, 2013.

Riebesell, U., Fabry, V. J., Hansson, L., and Gattuso, J.-P.: Guide to best practices for ocean acidification research and data reporting, Office for Official Publications of the European Communities 2011.

Riley, J. and Tongudai, M.: The major cation/chlorinity ratios in sea water, *Chemical Geology*, 2, 263-269, 1967.

705 Rushdi, A., Pytkowicz, R., Suess, E., and Chen, C.: The effects of magnesium-to-calcium ratios in artificial seawater, at different ionic products, upon the induction time, and the mineralogy of calcium carbonate: a laboratory study, *Geologische Rundschau*, 81, 571-578, 1992.

Schulz, K. G., Bach, L. T., Bellerby, R. G., Bermúdez, R., Büdenbender, J., Boxhammer, T., Czerny, J., Engel, A., Ludwig, A., and Meyerhöfer, M.: Phytoplankton blooms at increasing levels of atmospheric carbon dioxide: experimental evidence for negative effects on prymnesiophytes and positive on small picoeukaryotes, *Frontiers in Marine Science*, 4, 64, 2017.

710 Simkiss, K.: The inhibitory effects of some metabolites on the precipitation of calcium carbonate from artificial and natural sea water, *ICES Journal of Marine Science*, 29, 6-18, 1964.

Statista: Global cement industry - Statistics & Facts. See: <https://www.statista.com/topics/8700/cement-industry-worldwide/>, 2021.

Tang, H., Wu, X., Xian, H., Zhu, J., Wei, J., Liu, H., and He, H.: Heterogeneous Nucleation and Growth of CaCO<sub>3</sub> on Calcite (104) and Aragonite (110) Surfaces: Implications for the Formation of Abiogenic Carbonate Cements in the Ocean, *Minerals*, 10, 294, 2020.

715 The Royal Society and Royal Academy of Engineering.: Greenhouse Gas Removal. See: <https://royalsociety.org/-/media/policy/projects/greenhouse-gas-removal/royal-society-greenhouse-gas-removal-report-2018.pdf>, 2018.

Uppstrom, L.: The boron/chlorinity ratio of deep-sea water from the Pacific Ocean, *Deep Sea Res.*, 21, 161-162, 1974.

Wolf-Gladrow, D. A., Zeebe, R. E., Klaas, C., Körtzinger, A., and Dickson, A. G.: Total alkalinity: The explicit conservative expression and its application to biogeochemical processes, *Marine Chemistry*, 106, 287-300, 2007.

720 Wolf, S. E., Leiterer, J., Kappl, M., Emmerling, F., and Tremel, W.: Early homogenous amorphous precursor stages of calcium carbonate and subsequent crystal growth in levitated droplets, *Journal of the American Chemical Society*, 130, 12342-12347, 2008.

Wurgaft, E., Steiner, Z., Luz, B., and Lazar, B.: Evidence for inorganic precipitation of CaCO<sub>3</sub> on suspended solids in the open water of the Red Sea, *Marine Chemistry*, 186, 145-155, 2016.

725 Wurgaft, E., Wang, Z., Churchill, J., Dellapenna, T., Song, S., Du, J., Ringham, M., Rivlin, T., and Lazar, B.: Particle triggered reactions as an important mechanism of alkalinity and inorganic carbon removal in river plumes, *Geophysical Research Letters*, e2021GL093178, 2021.

Zeebe, R. E. and Wolf-Gladrow, D.: CO<sub>2</sub> in seawater: equilibrium, kinetics, isotopes, 65, Gulf Professional Publishing 2001.

Zhong, S. and Mucci, A.: Calcite and aragonite precipitation from seawater solutions of various salinities: Precipitation rates and overgrowth compositions, *Chemical geology*, 78, 283-299, 1989.

730

Table 1: Summary of experimental conditions. Please note that for comparability, more TA was added in the liquid than the sieved approaches to match the theoretical increases in calcium carbonate saturation state (see Methods section for details).

TA Agent	TA target ( $\mu\text{mol kg}^{-1}$ )	Comments	Amount added in mg (or mL*)	Amount of natural seawater in kg	mg $\text{kg}^{-1}$ (or mL $\text{kg}^{-1}$ *)	Theoretical Theoretical TA addition ( $\mu\text{mol kg}^{-1}$ )	Recorded TA addition ( $\mu\text{mol kg}^{-1}$ )	Experiment duration	Additional samples apart from TA and DIC
<b>Sieved calcium minerals experiments</b>									
CaO	250	Sieved in	15.50	2015.90	7.69	274.21	<u>216.49</u>	47 days	N/A
CaO	500	Sieved in	30.60	2004.50	15.27	544.42	<u>410.70</u>	47 days	TPC, POC and SEM samples
Ca(OH) <sub>2</sub>	250	Sieved in	19.90	2001.90	9.94	268.34	<u>221.96</u>	28 days	N/A
Ca(OH) <sub>2</sub>	500	Sieved in	37.40	2004.20	18.66	503.73	<u>440.19</u>	42 days	TPC, POC and SEM samples
<b>Na<sub>2</sub>CO<sub>3</sub>, particles and filtration experiments</b>									
Na <sub>2</sub> CO <sub>3</sub>	1050	1M Na <sub>2</sub> CO <sub>3</sub> solution	1.05*	2000.60	0.52	1050.32	<u>1057.41</u>	42 days	N/A
Na <sub>2</sub> CO <sub>3</sub>	1050	1M Na <sub>2</sub> CO <sub>3</sub> solution, plus quartz powder after 2 days Sieved in, filtered after 4 hours	1.05*	2000.30	0.5	1050.16	<u>1073.92</u>	48 days	TPC, POC and SEM samples
Ca(OH) <sub>2</sub>	500	filtered after 4 hours	39.30	2004.30	19.61	529.30	<u>470.79</u>	48 days	N/A
<b>Dilution experiments</b>									
Ca(OH) <sub>2</sub>	500	1:1 dilution after 10min, 1 hour, 1 day and 1 week	101.60	5132.50	19.80	534.36	<u>452.65</u>	14 days	TPC, POC and SEM samples
Ca(OH) <sub>2</sub>	2000	1:7 dilution after 10min, 1 hour, 1 day and 1 week	155.90	2003.80	77.80	2100.21	<u>724.04</u>	48 days	TPC, POC and SEM samples

Table 2: Comparison between the estimated PIC based on half the TA change between the theoretical maximum TA increase upon full dissolution of the alkaline material added and the measured TA at the end of the experiment (~~Table 1~~ **Table 4**), the estimated PIC based on half the TA changes between the measured maximum TA increase and the measured TA at the end of the experiment, and the measured PIC from the particulate carbon analysis.

Experiment	PIC $\Delta TA_{\text{Theo}}$ ( $\mu\text{mol kg}^{-1}$ )	PIC $\Delta TA$ ( $\mu\text{mol kg}^{-1}$ )	Measured PIC ( $\mu\text{mol kg}^{-1}$ )
500 TA – CaO- <del>Addition</del>	543.24	476.38	491.82 $\pm$ 39.18
500 TA – Ca(OH) <sub>2</sub> - <del>Addition</del>	462.28	430.51	550.87 $\pm$ 71.32
1050 TA – 1M Na <sub>2</sub> CO <sub>3</sub> - <del>Addition</del> + Quartz Particles	627.20	639.07	397.37 $\pm$ 24.03
500 TA – Ca(OH) <sub>2</sub> <del>Addition</del> <u>Dilution</u>	107.05	66.20	89.51 $\pm$ 4.27
2000 TA – Ca(OH) <sub>2</sub> <del>Addition</del> <u>Dilution</u>	1718.83	1030.74	1331.48 $\pm$ 50.73



Table 3: Simulations of the changes in TA, DIC,  $\Omega_{Ar}$ ,  $pCO_2$  and  $pH_T$  (total scale) after TA increases of 250, 500 and 1000  $\mu\text{mol kg}^{-1}$ , assuming complete mineral dissolution without precipitation, a complete dissolution followed by as much  $CaCO_3$  precipitated as the amount of TA added, and a complete dissolution followed by  $CaCO_3$  precipitation until reaching an  $\Omega_{Ar}$  of 2.0, before  $CO_2$  re-equilibration to initial  $pCO_2$ . For each scenario, the amount of moles of  $CO_2$  absorbed per moles of TA added has been calculated for comparison. The 500  $\mu\text{mol kg}^{-1}$  TA addition simulation is shown in [Figure A-3](#), Appendix. \*Note: the value for  $\Omega_{Ar}$  is rounded to 1.00 but calculated at 0.997.

	Starting Conditions (salinity = 35 19 °C)	TA +250 $\mu\text{mol kg}^{-1}$ No $CaCO_3$ precipitation	TA +500 $\mu\text{mol kg}^{-1}$		TA +1000 $\mu\text{mol kg}^{-1}$	
			No $CaCO_3$ Prec. = TA added	$CaCO_3$ Prec. until $\Omega_{Ar}$ of 2	No $CaCO_3$ Prec. = TA added	$CaCO_3$ Prec. until $\Omega_{Ar}$ of 2
TA ( $\mu\text{mol kg}^{-1}$ )	2350	2600	2850	1748	3350	1320
DIC ( $\mu\text{mol kg}^{-1}$ )	2100	2100	2100	1549	2100	1085
$\Omega_{Ar}$	2.80	5.53	8.45	2.00	14.57	2.00
$pCO_2$ ( $\mu\text{atm}$ )	416.2	175.1	91.5	319.2	29.6	144.81
$pH_T$	8.04	8.38	8.61	8.02	8.97	8.20
After re-equilibration, i.e., $pCO_2 \sim 416 \mu\text{atm}$						
Final TA ( $\mu\text{mol kg}^{-1}$ )	2350	2600	2850	1748	3350	1320
Final DIC ( $\mu\text{mol kg}^{-1}$ )	2100	2309	2517	1588	2926.5	1216
Final $\Omega_{Ar}$	2.80	3.34	3.90	1.66	5.14	1.00*
Final $pH_T$	8.04	8.08	8.11	7.93	8.17	7.82
$CO_2$ uptake (mole/mole TA)	NA	0.84	0.83	0.08	0.83	0.13

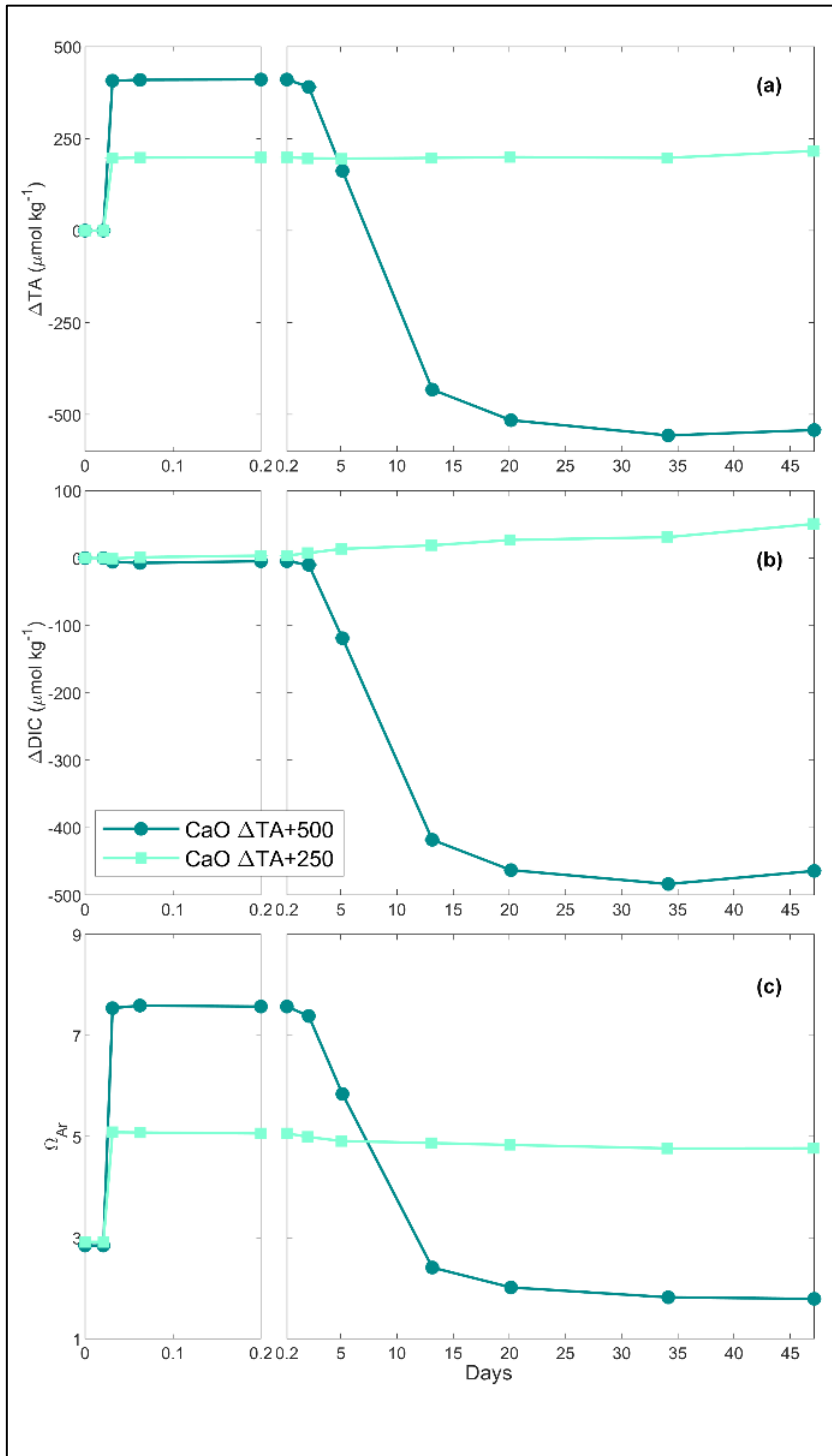
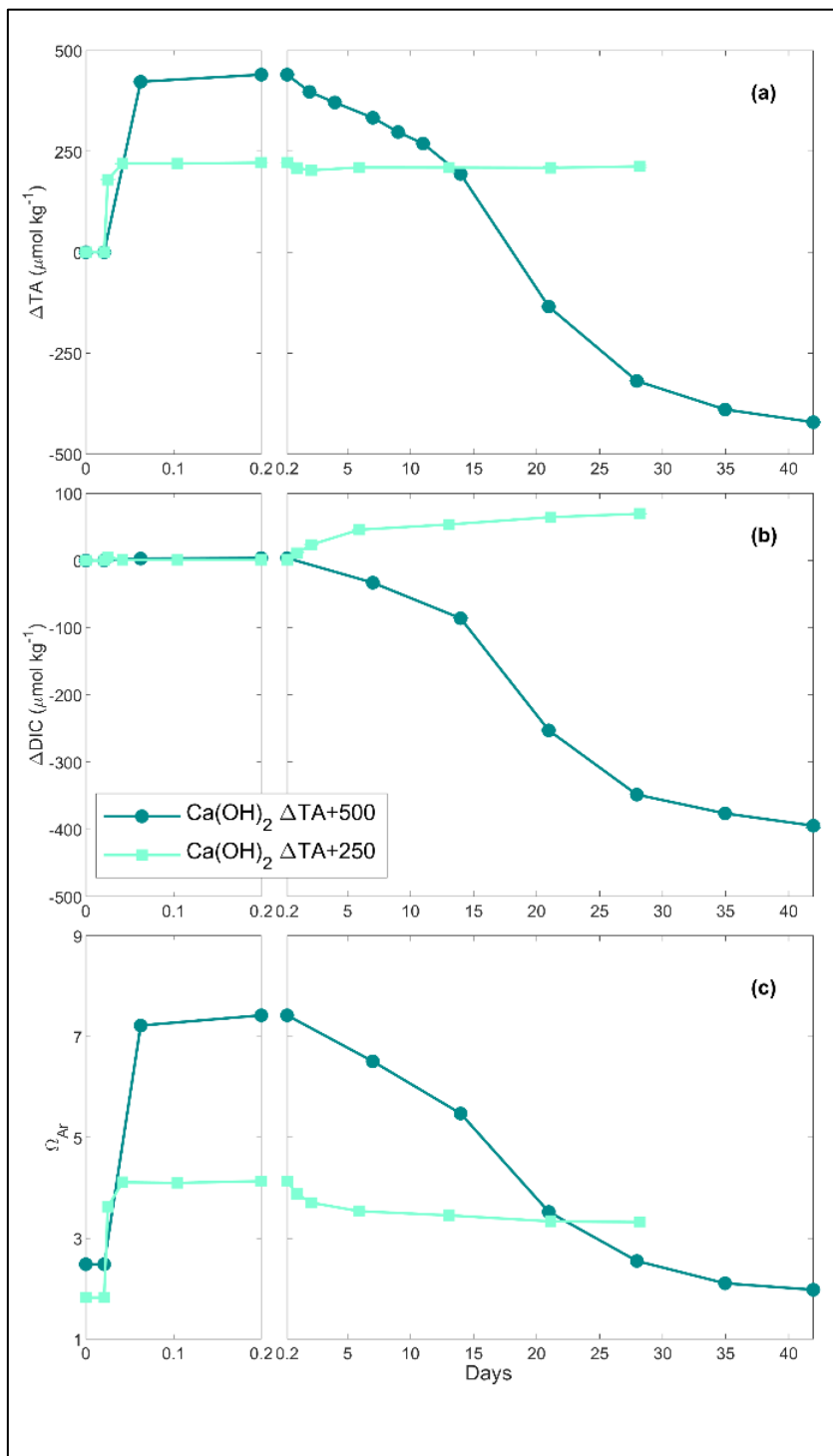
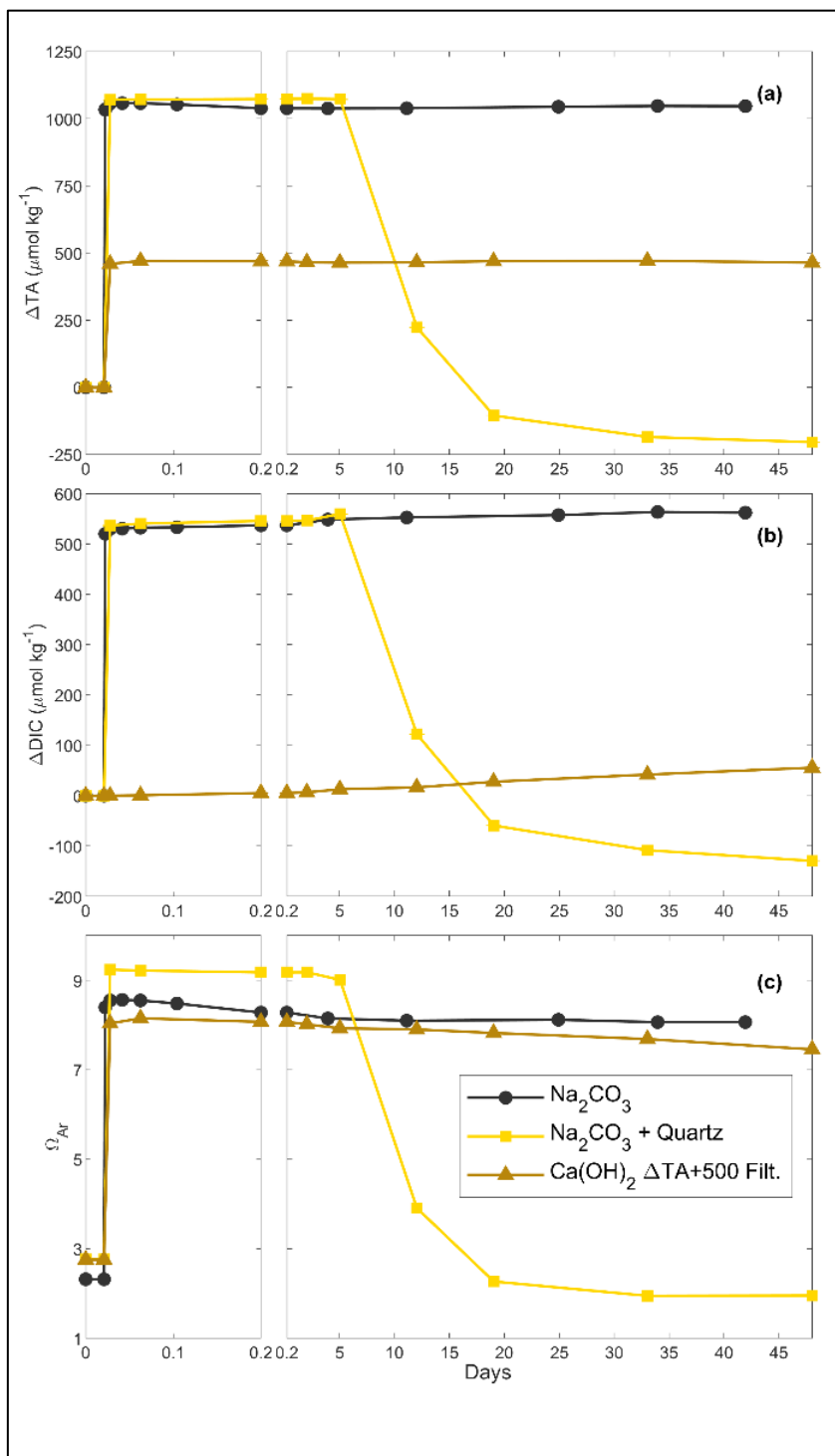


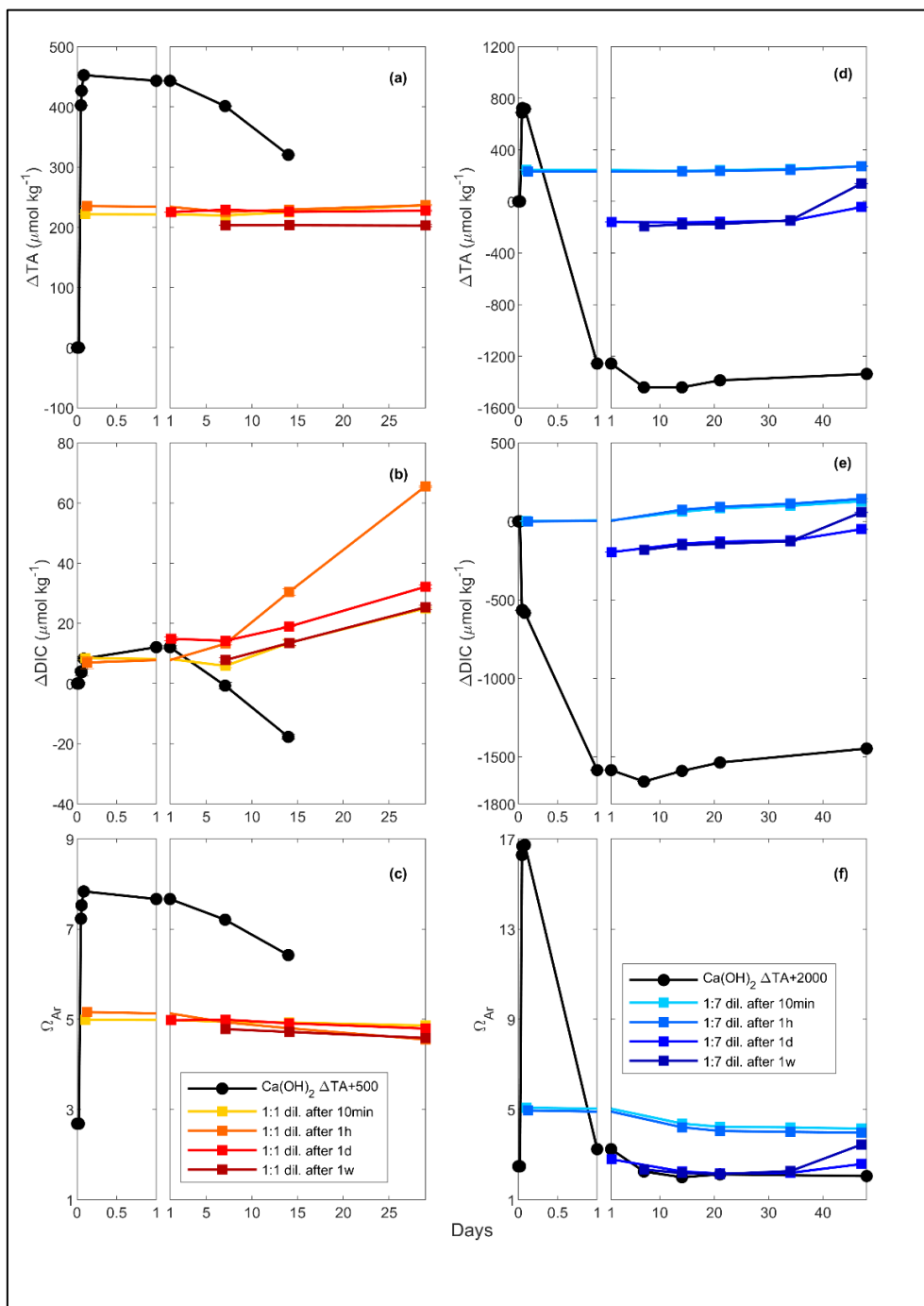
Figure 1: Changes in TA (a), DIC (b) and  $\Omega_{Ar}$  (c) over time following two CaO additions.



745 **Figure 2:** Changes in TA (a), DIC (b) and  $\Omega_{Ar}$  (c) of the samples over time following two  $\text{Ca}(\text{OH})_2$  additions.



**Figure 3: Changes in TA (a), DIC (b) and  $\Omega_{Ar}$  (c) over time following additions of  $\text{Na}_2\text{CO}_3$ ,  $\text{Na}_2\text{CO}_3$  plus quartz particles and  $\text{Ca}(\text{OH})_2$  followed by a filtration step (see Methods for details).**



750 **Figure 4:** Changes in TA (a and d), DIC (b and e) and  $\Omega_{\text{Ar}}$  (c and f) following a TA addition of 500 and 2000  $\mu\text{mol kg}^{-1}$  respectively, by  $\text{Ca}(\text{OH})_2$  (black line), as well as following a 1:1 dilution or the 500  $\mu\text{mol kg}^{-1}$  TA addition (red and yellow lines) and a 1:7 dilution for the 2000  $\mu\text{mol kg}^{-1}$  TA addition (blue lines). The dilutions were performed after 10 minutes, 1 hour, 1 day and 1 week and earlier dilutions are represented by lighter colours.

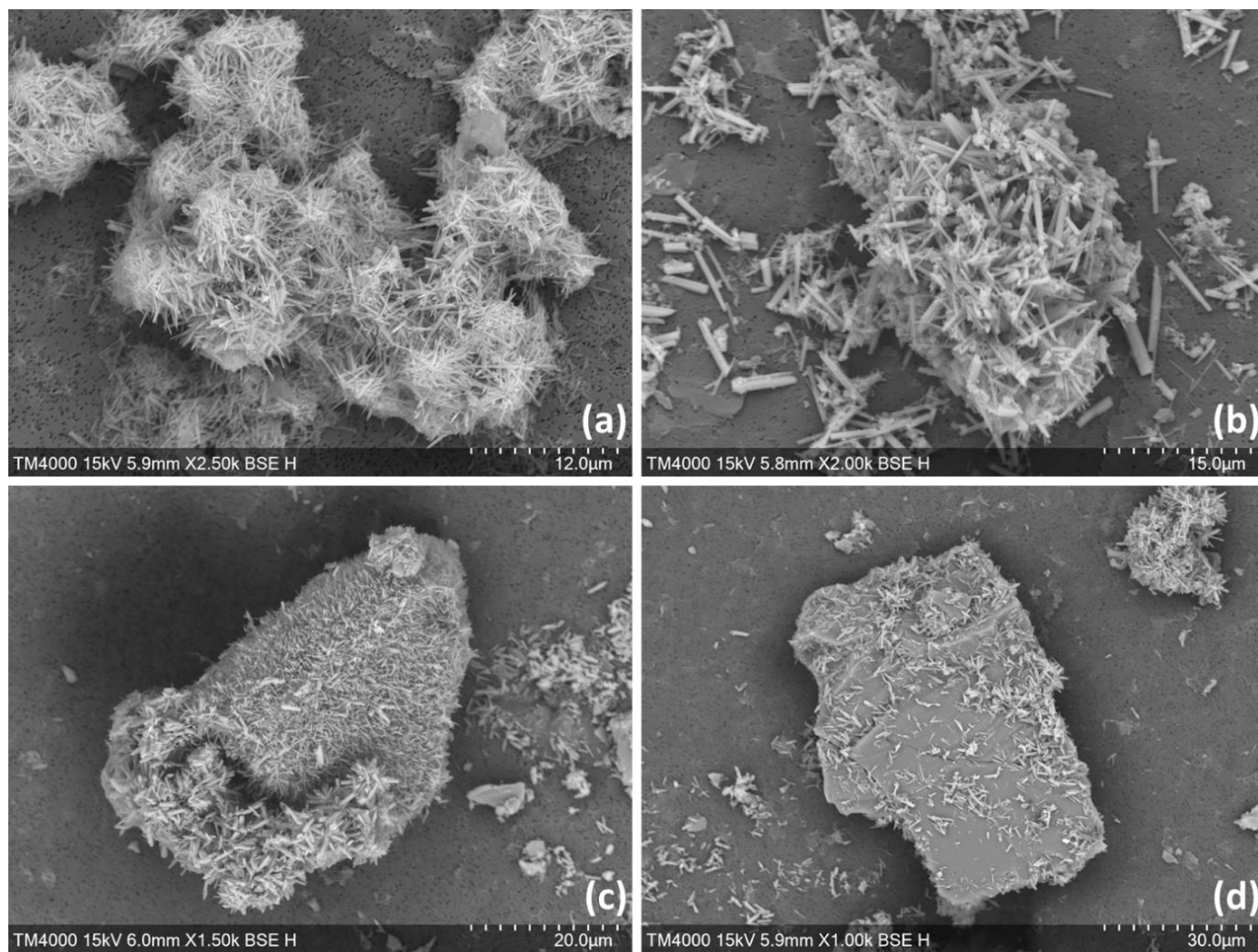


**Figure 5:** SEM images from experiments with an increase in TA of  $\sim 500 \mu\text{mol kg}^{-1}$  by CaO (a),  $\text{Ca(OH)}_2$  (b) and with a TA increase of  $\sim 1050 \mu\text{mol kg}^{-1}$  by 1M  $\text{Na}_2\text{CO}_3$ , followed by quartz particles addition ((c) and (d)).

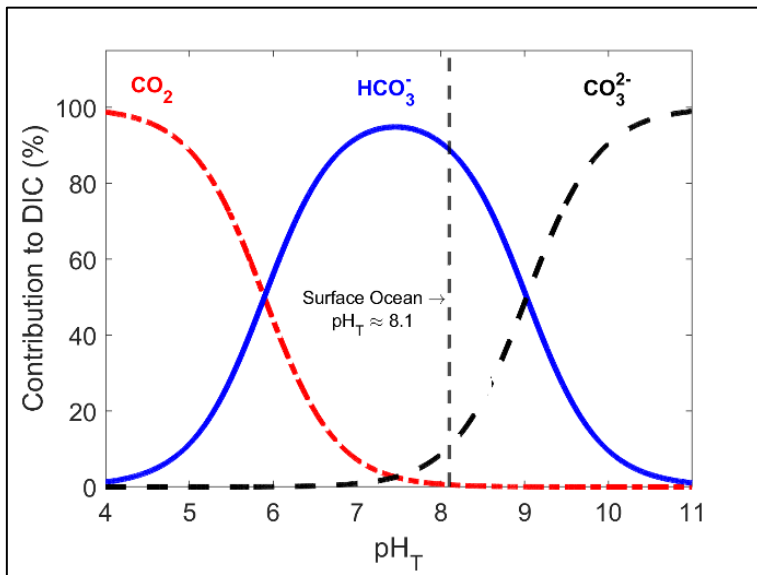
-Appendix

**Table A 1: Seawater salinity in each experiment, and phosphate concentrations in one of the batches (\*).**

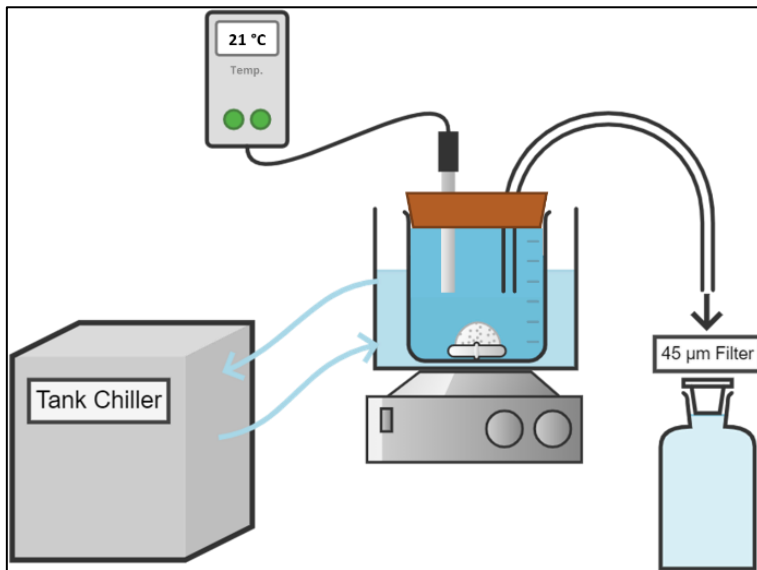
<u>Alkaline mineral</u>	<u>TA increase (in <math>\mu\text{mol kg}^{-1}</math>)</u>	<u>Experiment details</u>	<u>Seawater salinity</u>	<u>Phosphate (in <math>\mu\text{mol kg}^{-1}</math>)*</u>
<u>CaO</u>	<u>250</u>	<u>N/A</u>	<u>36.52</u>	<u>Not measured</u>
	<u>500</u>	<u>N/A</u>	<u>36.52</u>	<u>Not measured</u>
<u>Ca(OH)<sub>2</sub></u>	<u>250</u>	<u>N/A</u>	<u>36.91</u>	<u>Not measured</u>
	<u>500</u>	<u>N/A</u>	<u>36.91</u>	<u>Not measured</u>
	<u>500</u>	<u>For dilutions</u>	<u>35.46</u>	<u>Not measured</u>
	<u>500</u>	<u>For filtration</u>	<u>36.52</u>	<u>Not measured</u>
	<u>2000</u>	<u>For dilution</u>	<u>36.74</u>	<u>0.32 <math>\pm</math>0.03</u>
<u>Na<sub>2</sub>CO<sub>3</sub></u>	<u>1050</u>	<u>N/A</u>	<u>36.91</u>	<u>Not measured</u>
	<u>1050</u>	<u>With quartz particles</u>	<u>36.52</u>	<u>Not measured</u>

765 **Table A 21: Main chemical composition of the CaO and Ca(OH)<sub>2</sub> ~~powders~~ feedstocks used for the TA increase experiments determined by ICPMS analysis.**

<u>CaO Powder</u>			<u>Ca(OH)<sub>2</sub> Powder</u>		
<u>Element</u>	<u>mg g<sup>-1</sup></u>	<u>St. Dev.</u>	<u>Element</u>	<u>mg g<sup>-1</sup></u>	<u>St. Dev.</u>
Calcium	545.15	70.92	Calcium	529.79	117.30
Magnesium	2.10	0.23	Magnesium	6.87	1.98
Silicon	2.02	1.79	Silicon	2.70	1.12
Aluminium	0.50	0.19	Aluminium	1.98	0.77
Iron	0.32	0.10	Iron	0.91	0.34
Manganese	0.11	0.01	Potassium	0.43	0.23
Potassium	0.03	0.00	Titanium	0.07	0.03
Phosphorus	0.02	0.02	Manganese	0.05	0.01
Titanium	0.02	0.01	Phosphorus	0.04	0.01
Chromium	0.01	0.01	Bromine	0.03	0.01



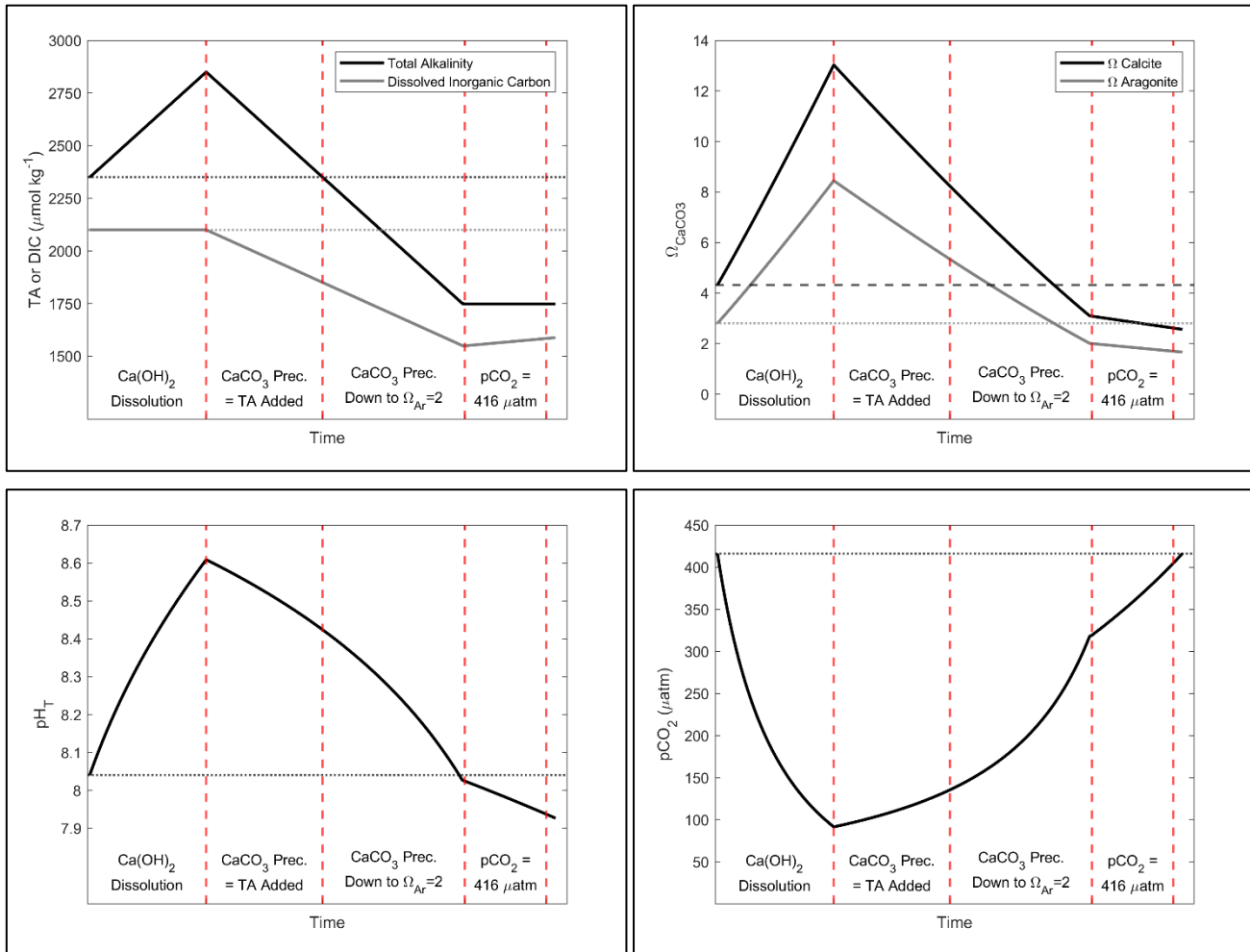
770 **Figure A 1: Relative contribution of dissolved CO<sub>2</sub>, HCO<sub>3</sub><sup>-</sup> and CO<sub>3</sub><sup>2-</sup> to total dissolved inorganic carbon in seawater as a function of pH<sub>T</sub> (total scale), also known as Bjerrum plot (based on the carbonic acid equilibrium constant from Mehrbach et al. (1973) and refitted by Dickson and Millero (1987)), at 25 °C and salinity of 35, with the current surface ocean pH average represented by the dashed line (pH<sub>T</sub> ~8.1).**



775 **Figure A 2: Conceptual diagram of the experimental setup used for the dissolution of alkaline minerals**



780



785

**Figure A 3: Simulation of the changes in TA, DIC,  $\Omega_{\text{Ca}}$ ,  $\Omega_{\text{Ar}}$ ,  $\text{pCO}_2$  and  $\text{pH}_T$  after addition of  $500 \mu\text{mol kg}^{-1}$  of alkalinity. Four important steps are presented: first-First, assuming the complete  $\text{Ca(OH)}_2$  dissolution without  $\text{CaCO}_3$  precipitation, second, assuming as much  $\text{CaCO}_3$  precipitation as the amount of TA added, third, assuming  $\text{CaCO}_3$  precipitation happening until reaching an  $\Omega_{\text{Ar}}$  = of 2.0, and fourth,  $\text{CO}_2$  uptake until equilibrium is reached between atmospheric-atmosphere and seawater at a  $\text{pCO}_2$  of ~416  $\mu\text{atm}$ .**

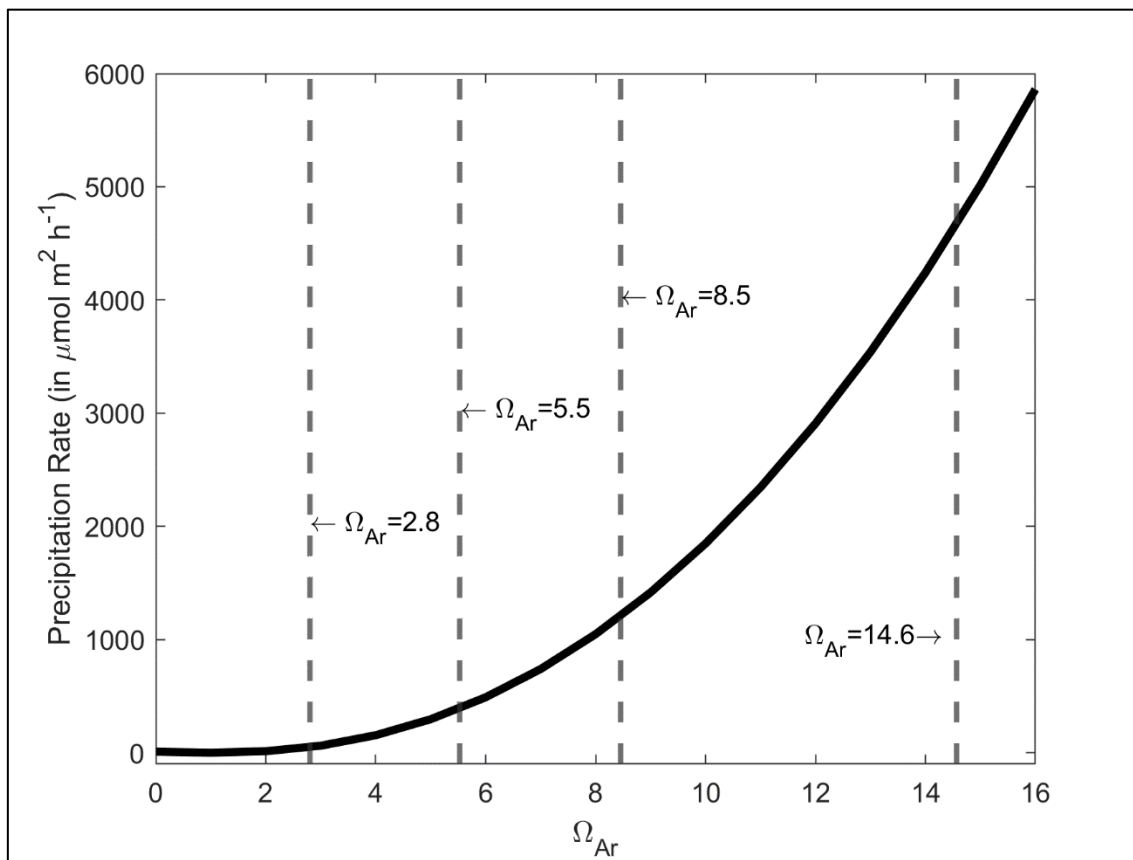
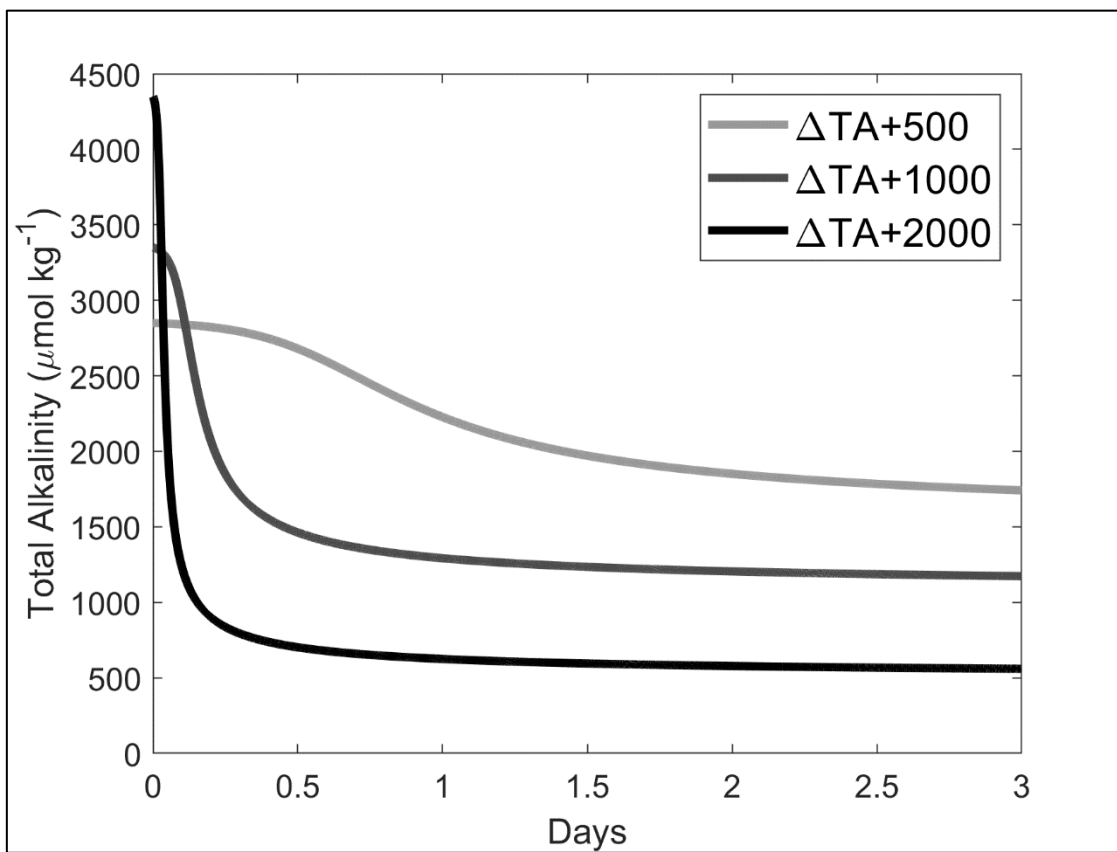


Figure A 4: CaCO<sub>3</sub> Aragonite precipitation rate onto CaCO<sub>3</sub> aragonite seed crystals in  $\mu\text{mol m}^{-2} \text{h}^{-1}$  as a function of  $\Omega_{Ar}$ , based on the calculation-measurements of Zhong and Mucci (1989) at 25 °C and for a salinity of 35. The values of  $\Omega_{Ar}$  values for the starting conditions, and following a +250, +500 and +1000  $\mu\text{mol kg}^{-1}$  TA increase are presented by the grey dashed lines, i.e., 2.8, 5.5, 8.5 and 14.6 respectively.

790



795

**Figure A 5: Simulations of TA loss due to aragonite precipitation after a TA addition of 500, 1000 and 2000  $\mu\text{mol kg}^{-1}$ , based on  $\Omega_{Ar}$  and surface area dependant precipitation rates shown in Figure A 4, Zhong and Mucci (1989) assuming the initial presence of 2% of  $\text{CaCO}_3$  in our samples, i.e.,  $\sim 0.37$ ,  $\sim 0.74$  and  $\sim 1.48 \text{ mg kg}^{-1}$  for a  $\Delta\text{TA}+500$ ,  $\Delta\text{TA}+1000$  and  $\Delta\text{TA}+2000 \mu\text{mol kg}^{-1}$ , respectively.  $\text{CaCO}_3$  mass was converted to a surface area as described in Zhong and Mucci (1989). The starting conditioned were  $\text{TA} = 2300 \mu\text{mol kg}^{-1}$ ,  $\text{DIC} = 2100 \mu\text{mol kg}^{-1}$ , salinity = 35 and temperature =  $21 \text{ }^\circ\text{C}$ .**